

See discussions, stats, and author profiles for this publication at: <https://www.researchgate.net/publication/243969715>

Recent Advances in Design and Fabrication of Upconversion Nanoparticles and Their Safe Theranostic Applications

ARTICLE in ADVANCED MATERIALS · JULY 2013

Impact Factor: 17.49 · DOI: 10.1002/adma.201301197 · Source: PubMed

CITATIONS

105

READS

234

6 AUTHORS, INCLUDING:



Zhanjun Gu

Chinese Academy of Sciences

82 PUBLICATIONS 2,030 CITATIONS

[SEE PROFILE](#)



Gan Tian

Sichuan University

36 PUBLICATIONS 1,017 CITATIONS

[SEE PROFILE](#)



Shoujian Li

Sichuan University

74 PUBLICATIONS 1,354 CITATIONS

[SEE PROFILE](#)



Yuliang Zhao

Chinese Academy of Sciences

345 PUBLICATIONS 11,824 CITATIONS

[SEE PROFILE](#)

Recent Advances in Design and Fabrication of Upconversion Nanoparticles and Their Safe Theranostic Applications

Zhanjun Gu, Liang Yan, Gan Tian, Shoujian Li, Zhifang Chai, and Yuliang Zhao*

Lanthanide (Ln) doped upconversion nanoparticles (UCNPs) have attracted enormous attention in the recent years due to their unique upconversion luminescent properties that enable the conversion of low-energy photons (near infrared photons) into high-energy photons (visible to ultraviolet photons) via the multiphoton processes. This feature makes them ideal for bioimaging applications with attractive advantages such as no autofluorescence from biotissues and a large penetration depth. In addition, by incorporating advanced features, such as specific targeting, multimodality imaging and therapeutic delivery, the application of UCNPs has been dramatically expanded. In this review, we first summarize the recent developments in the fabrication strategies of UCNPs with the desired size, enhanced and tunable upconversion luminescence, as well as the combined multifunctionality. We then discuss the chemical methods applied for UCNPs surface functionalization to make these UCNPs biocompatible and water-soluble, and further highlight some representative examples of using UCNPs for *in vivo* bioimaging, NIR-triggered drug/gene delivery applications and photodynamic therapy. In the perspectives, we discuss the need of systematically nanotoxicology data for rational designs of UCNPs materials, their surface chemistry in safer biomedical applications. The UCNPs can actually provide an ideal multifunctionalized platform for solutions to many key issues in the front of medical sciences such as theranostics, individualized therapeutics, multimodality medicine, etc.

1. Introduction

The nanoparticles (NPs) based bright, tissue-specific imaging probes are being developed to visualize, characterize and

Prof. Z. Gu, Dr. L. Yan, Dr. G. Tian, Prof. Y. Zhao
CAS Key Laboratory for Biomedical Effects of
Nanomaterials and Nanosafety
National Center for Nanosciences and Technology of
China and Institute of High Energy Physics
Chinese Academy of Sciences (CAS)
Beijing, China
E-mail: zhaojuliang@ihep.ac.cn

Dr. G. Tian, Prof. S. Li
College of Chemistry
Sichuan University
Chengdu 610064, China
Prof. Z. Chai
School of Radiation Medicine and Radiation Protection
Soochow University
Suzhou 215123, China

DOI: 10.1002/adma.201301197



quantify biological processes at a cellular and molecular level in a non-invasive manner, which enables accurate diagnosis and individualized treatment of various diseases such as cancer.^[1–9] At the meantime, NPs are being used as drug carriers by careful construction of nanostructure and surface modification. The NPs-based drug delivery systems not only improve the treatment efficacy but also reduce the side-effects.^[6,10,11] Moreover, these imaging and delivery facilities have been successfully combined into unique NPs platforms through the delicate combinations of various functional components, enabling simultaneous *in vivo* diagnostic imaging and drug delivery for real-time treatment tracking.

Among the broad spectrum of nanomaterials being investigated for biomedical applications, upconversion nanoparticles (UCNPs) (mainly lanthanide (Ln)-doped rare-earth NPs) have attracted significant attention due to their intrinsic upconversion luminescent properties, providing many uncommon opportunities in biomedical applications.^[6,12–20] First, compared with the conventional fluorescent

materials (such as organic dyes and semiconductor quantum dots (QDs)), Ln-doped UCNPs have the ability to absorb and convert near infrared light (NIR) to visible/UV light efficiently through an upconversion process, which leads to many unique advantages for optical imaging and bioassay, such as low background autofluorescence, deep light penetration depth, minimal photo-damage to living organisms, etc.^[6,21–31] Thus, upconversion luminescence (UCL) imaging *in vivo* is expected to be the next-generation photoluminescence imaging technique since it provides high sensitivity and spatial resolution. Second, UCNPs have moved into the spotlight as an efficient platform for constructing multifunctional nanoprobes.^[9,32,33] Due to the similar ionic radii and chemical properties of Ln ions, doping is a very common method to incorporate the different functional Ln ions in the UCNPs for desired multifunctional properties. For example, Gd based/doped UCNPs have been used as dual-modality contrast agents for magnetic resonance imaging (MRI) and optical imaging.^[34,35] Gd-, Yb-, and Lu-doped UCNPs with higher atomic number and stronger X-ray attenuation have been served as excellent computed

tomography (CT)/MRI/optical contrast agents.^[36,37] In addition, radionuclides, such as the ¹⁸F and ¹⁵³Sm, with positron emission tomography (PET) or single-photon emission computed tomography (SPECT) imaging capability could also be easily introduced into the lattice of UCNPs.^[38,39] As a result, multimodal imaging techniques integrating UCL imaging with different imaging modalities have been rapidly developed, which may help the medical imaging to be more sensitive and accurate. Third, apart from their multiple imaging capabilities, UCNPs are also ideally suited to be applied as drug delivery systems, making the development of a new generation of theranostic agents.^[40–45] The most successful therapeutic applications of UCNPs mainly focused on the NIR triggered photodynamic therapy (PDT) in deep tissues. Under NIR light excitation, UCNPs are able to emit visible light which can activate surrounding photosensitizer (PS) molecules to produce singlet oxygen (¹O₂) and then kill cancer cells. In addition, owing to their versatile surface functionality, chemotherapeutic/biotherapeutic agents could be also loaded onto the UCNPs surface for targeted delivery and controlled release. Finally, UCNPs are also biocompatible since they do not contain toxic elements, thus offering them great potentials for the use in biomedical fields. Due to these distinctive advantages, recent years have witnessed the rapid pace of research and development of UCNPs for biomedical applications (Figure 1). Therefore, though many outstanding reviews have devoted to different aspects of UCNPs field, it is still significant to make a new summarization of the most recent advances in rational design and synthesis of Ln-doped UCNPs as well as their biomedical applications.

In this review, we focus primarily on the progresses of biomedical UCNPs in the past five years, some newly developed strategies for their surface functionalization, and their theranostic applications. Rather than attempting to provide a complete historical survey, our emphasis here is on discussions that could offer future opportunities to create new properties or enhance the functionality of UCNPs materials. The present review contains five sections. First, we present the basic considerations for how to fabricate the efficient and biocompatible UCNPs such as dopant/host selection criteria, synthesis route, upconversion emission tuning, and the toxicity of currently used materials. A series of strategies for the surface modification of UCNPs to improve their water-dispersity, biocompatibility and specific targeting capabilities, are summarized in section 2. The application of UCNPs for biomedical imaging especially the UCNPs based multicolor and multimodal imaging *in vivo* are discussed in section 3. The section 4 mainly discusses the applications of UCNPs for cancer therapy, including PDT and NIR triggered chemotherapeutic agents/gene delivery. The final section frames the future outlook for UCNPs by highlighting areas of exceptional promise and challenges.

2. Upconversion Nanoparticle Design Considerations

2.1. Dopant/Host Selection Criteria

UCNPs are generally comprised of an inorganic host matrix doped with light absorbers (sensitizer) and light-emitting ions



Zhanjun Gu received his BE degree (2002) from Huazhong University of Science and Technology and PhD degree (2007) from Institute of Chemistry, Chinese Academy of Science (CAS), under the direction of Prof. Jiannian Yao. He then became a postdoctoral fellow at university of Georgia. In 2009, he joined the faculty at CAS Key Lab for Biomedical Effects of Nano-materials & Nanosafety of the Institute of High Energy Physics, CAS. His current research interests include nanomaterials synthesis, optical spectroscopy and bio-applications of luminescent nanomaterials.



Liang Yan is a graduate student of CAS Key Lab for Biomedical Effects of Nano-materials & Nanosafety. He received his BSc in Chemistry at Sichuan University in 2009. Since then he studied as a PhD under the direction of Prof. Yuliang Zhao. He is now studying chemical functionalization and biological applications of graphene and upconversion nanomaterials as well as their biomedical effects.



Gan Tian graduated with a B.Sc. from the Sichuan University in 2009. He is currently a Graduate student at the College of Chemistry of Sichuan University under the co-supervision of Prof. Shoujian Li and Prof. Yuliang Zhao. His research topic is the fabrication and biomedical application of luminescent nanomaterials.



Shoujian Li received his PhD in radiochemistry chemistry at Sichuan University. He is the head of the research group "Functional Materials for Radionuclides Separation" of the Chemistry College of Sichuan University. His research mainly includes the design and synthesis of new functional carbonaceous materials, advanced materials and technologies for spent fuel reprocessing, treatment and disposal of nuclear wastes, including the uses of carbon nanomaterials.



Zifang Chai received the Bachelor Degree at Fudan University in 1964. He became the Director of Department of Nuclear Chemistry in 1983, and full Professor in 1988 at Institute of High Energy Physics, Chinese Academy of Sciences. He was elected as the Member of Chinese Academy of Sciences in 2007.



Yuliang Zhao is the founder of CAS Key Lab for Biomedical Effects of Nano-materials & Nanosafety, and Professor and Deputy Director-General of National Center for Nanoscience and Technology of China. His research interests mainly include Nanotoxicological Chemistry, Radiochemistry and MD Simulations of biochemical processes on nano/bio interface.

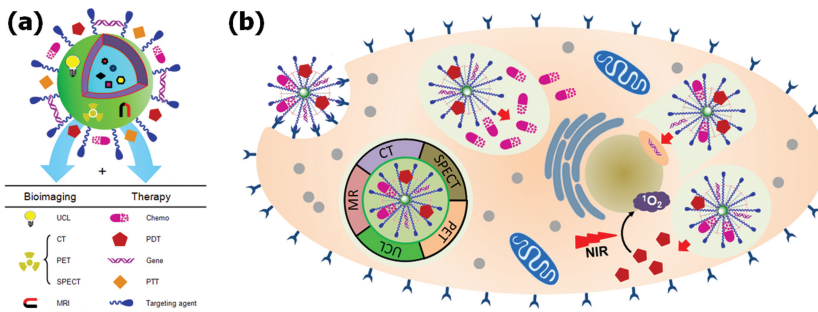


Figure 1. (a) Graphic illustration of the structure of multifunctional/multimodal UCNPs. (b) Illustration of potential applications of multifunctional imaging/therapeutic UCNPs at the cellular level.

(the activator) (Figure 2). Among the available types of activators, Ln^{3+} ions (mainly Er^{3+} , Tm^{3+} and Ho^{3+}) have been the primary activator choice in UCNPs because of their ladder-like arranged energy levels that promote upconversion by the absorption of multiple photons.^{[46–49] They also have large gaps between energy states that discourage nonradiative energy transfer among various excited levels of the ions. To enhance upconversion efficiency, Yb^{3+} with a larger absorption cross-section in the NIR spectral region is frequently doped as a sensitizer in combination with the activators. Selection of appropriate host materials is also essential in the synthesis of Ln -doped nanocrystals}

with desired nanoscale characteristics and favorable optical properties such as high upconversion efficiency and controllable emission profiles. An ideal host matrix needs to be easily obtained with small size, uniform shape and narrow size distribution. Moreover, its lattice phonon energies must be low since host lattice with low phonon energies minimizes nonradiative losses and maximize the radiative emission.^[48] To readily incorporate Ln dopant ions, it also requires host materials have close lattice matched to dopant ions. Based on these criteria, the most commonly used host material for the fabrication of UCNPs are rare earth fluorides including binary REF_3 and complex AREF_4 (RE = rare earth, A = alkali).^[33,50–55] For instance, Yb/Er or Yb/Tm co-doped hexagonal NaYF_4 nanocrystals have been identified as the most efficient UCNPs. The application of NaYF_4 -based UCNPs in biomedicine is increasing rapidly and offers excellent prospects for the development of new non-invasive strategies for the bioimaging *in vivo* and cancer therapy. However, the explorations of new materials as host matrix for UCNPs to obtain better performance or desired nanoscale characteristics never stop. For example, one of the most challenges of NaYF_4 -based UCNPs as bioprobes for biological applications is that it is hard to obtain ideal nanocrystals with smaller size (less than 10 nm) and

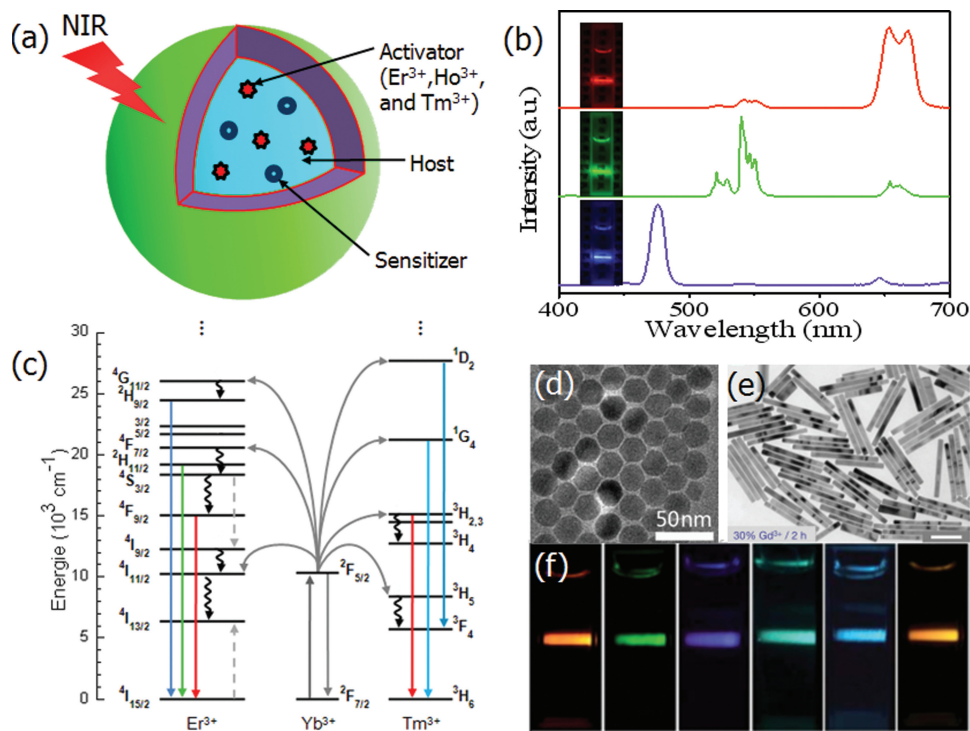


Figure 2. Structure and optical properties of UCNPs: (a) Scheme illustration of the structure and components of the UCNPs. (b) Typical emission spectra of $\text{Yb}/\text{Er}(\text{Tm})$ co-doped NaYF_4 UCNPs. Inset: their corresponding luminescent photographs under 980-nm NIR excitation. (c) Proposed energy transfer mechanisms exhibiting the upconversion processes in Er^{3+} , Tm^{3+} , and Yb^{3+} doped crystals under 980-nm excitation. TEM images of Mono-disperse (d) $\text{NaYF}_4:\text{Yb}/\text{Er}$ nanoplates and (e) Gd-doped $\text{NaYF}_4:\text{Yb}/\text{Er}$ nanorods. (f) Multicolor fine-tuning through the use of GdVO_4 UCNPs with different dopant ions or varying dopant ratios. Adapted with permission.^[73,76,105] Copyright 2010 and 2012, Nature Publishing Group and Royal Society of Chemistry.

brighter UCL. To overcome this problem, other fluorides such as $\text{Na}_x\text{ScF}_{3+x}$,^[56] NaYbF_4 ,^[57] KGdF_4 ,^[58] CaF_2 ,^[59,60] NaLuF_4 ,^[61–63] and BaLuF_5 ^[64] are recently becoming popular choices as host materials to fabricate smaller and brighter UCNPs. In order to obtain special optical properties, YO_2 ,^[65] KMnF_3 ,^[27] and NaMnF_3 ^[66] are developed as host materials to obtain single band UCL. Very recently, for constructing multifunctional UCNPs, hybrid host materials such as $\text{Gd}^{[35,67]}$ $\text{Mn}^{[28]}$,^[28] ^{18}F ^[38,68] and ^{153}Sm ^[39,69,70] doped NaREF_4 ($\text{RE} = \text{Y, Yb, and Lu}$) have been developed as excellent CT/MRI/PET/optical contrast agents.

2.2. Synthesis of Upconversion Nanoparticles

For Ln-doped UCNPs to be utilized as a promising bioprobe, they should possess characteristics of appropriate size and shape, suitable surface functional groups, high luminescent efficiency as well as low toxicity to living systems. To meet these requirements, many techniques especially “wet chemical method” have been developed to address the specific needs of UCNPs with tailored crystal size, morphology, chemical composition, surface functionalization, and optical properties. In the following part, we will discuss some of the recent successful approaches to date for synthesizing UCNPs.

Hydrothermal method is believed to be an effective water-based method for the fabrication of well-crystallized UCNPs under relative low temperature. The most advantage of this approach is that it can prepare various kinds of UCNPs, such as oxide,^[71,72] vanadate,^[73] phosphate,^[74–76] fluoride^[33,54,77] and oxysulfide^[78] with the fine control of size, shape and structures. In addition, some complicated structures, such as urchin-like hollow spheres,^[79] rattle-type architectures^[80] and hollow nanospheres with mesoporous shell,^[81] are also obtained by hydrothermal synthesis, while these structures are not easy to be prepared by other synthetic approaches. Furthermore, during the process of hydrothermal reaction, various commercially available ligands such as polyethylene glycol (PEG),^[82] polyvinylpyrrolidone (PVP),^[78,83] polyethylenimine (PEI),^[84] ethylenediaminetetraacetic acid (EDTA),^[85] cetyltrimethylammonium bromide (CTAB),^[86] and trisodium citrate (TSC)^[87] were widely used to control particle growth and endow them with water-dispersity and surface functionality. Especially, the PEI-coated UCNPs have a lot of $-\text{NH}_2$ functional groups for direct surface functionalization of biomolecules.^[84] However, by using hydrothermal synthesis, it is hard to produce ultra-small (less than 10 nm) and monodispersed nanocrystals.

Alternatively, the thermal decomposition and solvothermal method have proved to be powerful in the fabrication of UCNPs with monodispersed size, high crystallinity and bright UCL, and thus are the two most widely adopted methods for high quality UCNPs synthesis especially for fluorides. Murray's group,^[88–92] Yan's group,^[93,94] Capobianco's group^[95–97] and many other researchers^[57,61] have reported that highly monodispersive and uniform NaYF_4 , NaGdF_4 , NaLuF_4 and $\text{KY}_3\text{Ti}_2\text{O}_{10}$ UCNPs as well as other various fluoride can be prepared via the thermal decomposition and solvothermal approaches in high boiling organic solvent (such as OA/OM/1-octadecene). Furthermore, recently, many modified thermal decomposition/solvothermal approaches have been emerging to prepare

UCNPs with better performance or desired nanostructures. For example, in their recent work, Murray and co-workers improved the thermal decomposition method by using high heating rates up to 100 °C/min to synthesize NaYF_4 UCNPs with a remarkably narrow size distribution without the need for size-selective fractionation.^[91] Two/multi-step thermal decomposition are also developed for constructing core-shell structure of UCNPs.^[83,98–104] In the first step, UCNPs cores are prepared through the thermal decomposition. Then, these cores are used as seeds and a homogenesis or heterogeneous layer epitaxially grows around the cores to form core-shell structure via the similar procedure. This homogenesis or heterogeneous shell not only efficiently enhances the intensity of upconversion emission but also incorporates new functionalities by inducing functional components. Importantly, up to date, the two/multi-step thermal decomposition/solvothermal method is the only way to produce such core/shell structured UCNPs. To shorten the reaction time and increase the crystal quality, microwave-assisted solvothermal method and ionic liquid-based approach are employed to create small size, highly crystalline, and strongly luminescent UCNPs at a lower temperature.^[51,55]

However, to obtain desired size, crystal phase and optical properties of UCNPs, the above-mentioned strategies have to simultaneously control over a set of experimental parameters such as temperature, reaction time, solvent and concentration of precursors. To simplify the synthetic procedure, Liu et al.^[105] developed a novel Gd-doping assisted solvothermal method in which Gd^{3+} ions doping influenced the growth process of NaYF_4 UCNPs to give simultaneous control over the crystallographic phase, size and optical emission properties of the resulting nanocrystals (Figure 3). In contrast to conventional synthetic methods that require the fine control over several experimental factors for controlling crystallite size and phase, the Gd-doping approach requires the modification of only a single experimental parameter (dopant concentration), while enabling tremendous improvements in controlling the formation of UCNPs with small size, and desirable optical properties. This Gd-doping method has been extended to synthesize other UCNPs such as MF_2 ($\text{M} = \text{Ca, Sr and Ba}$) nanocrystals.^[106] More recently, we also developed a Mn-doping assisted solvothermal method for the synthesis of NaYF_4 nanocrystals with fine-tuned phase (from hexagonal to cubic), size (down to ~20 nm) and upconversion emission color (from green to red).^[28]

2.3. Optical Properties Tuning

Enhancement of upconversion luminescence efficiency: For biological studies and clinical applications, the UCL efficiency is of critical importance because the high UCL efficiency can improve the signal-noise-ratio. Hexagonal phase NaYF_4 is known as the most efficient host for upconversion emission, which is as brighter as 1 order compared to its cubic phase. However, the as-prepared NaYF_4 UCNPs with bright UCL usually have related-big size that is not favorable for their biological application. Therefore, three main routes have been developed to enhance the emission efficiency of upconversion while avoid the increase of particle size. First, doping impurities (such as alkaline, alkaline-earth ions, Gd^{3+} , Ti^{4+} , Mn^{2+} etc.) into the host

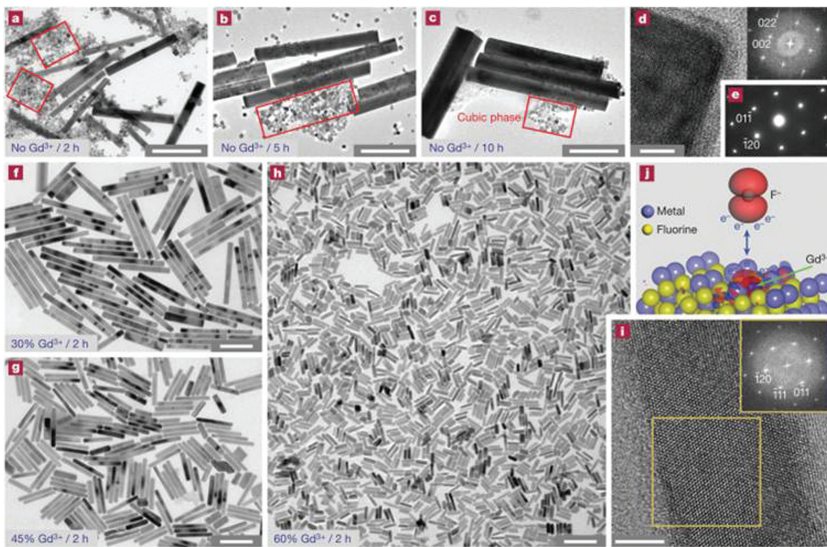


Figure 3. TEM characterization of $\text{NaYF}_4:\text{Yb}/\text{Er}$ nanocrystals doped with various concentrations of Gd^{3+} ions: (a-c) TEM images of $\text{NaYF}_4:\text{Yb}/\text{Er}$ nanoparticles obtained after heating for 2, 5 and 10 h in the absence of Gd^{3+} dopant ions. (d) High-resolution TEM image taken in [100] incidence and the corresponding Fourier-transform diffractogram (inset). (e) Electron diffraction pattern taken in [211] incidence of a nanorod in the mixture. (f-h) TEM images of $\text{NaYF}_4:\text{Yb}/\text{Er}$ nanoparticles obtained after heating for 2 h in the presence of 30, 45 and 60 mol% Gd^{3+} dopant ions, respectively. (i) High-resolution TEM image taken in [211] incidence and the corresponding Fourier-transform diffractogram (inset) of a nanorod. (j) DFT calculation showing the change of surface charge density. Scale bars are 500 nm for panels a-c, 200 nm for panels f-h and 5 nm for panels d and i. Adapted with permission.^[105] Copyright 2010, Nature Publishing Group.

matrix is a useful method to greatly enhance the UCL emission intensity.^[28,53,54,105,107] Recently, Wang et al.^[105] and Chen et al.^[107] reported that doping with Gd^{3+} or Ti^{4+} into NaYF_4 matrixes led to induce cubic-to-hexagonal phase transition of $\text{NaYF}_4:\text{Yb}/\text{Er}$ nanocrystals, which greatly enhanced the intensity of UCL. In addition, the impurities doping also decreases the crystal size, facilitating their bioapplications. Another useful strategy for the enhancement of the UCL intensity is to attach Ag or Au NPs onto UCNPs surfaces.^[108–110] This enhancement of UCL is attributed to the surface-plasmon-coupled emission, which can increase the radiative decay rate and emission efficiency. Recently, the most widely used strategy to improve the luminescence of UCNPs is the fabrication of core-shell structures where a shell with similar lattice constant with the core is grown around the UCNPs. In such core-shell structures, the dopant ions are confined in the interior core of the nanocrystals. The shell could effectively suppress energy loss on the crystal surface, leading to enhance luminescence efficiency. More and more core-shell nanocomposites, such as $\text{NaYF}_4:\text{Yb}/\text{Er}(\text{Tm})@\text{NaYF}_4$,^[111] $\text{NaYF}_4:\text{Yb}/\text{Er}@\text{NaGdF}_4$,^[112] $\text{NaGdF}_4:\text{Yb}/\text{Er}@\text{NaGdF}_4$,^[113] $\text{LaF}_3:\text{Tm}@\text{LaF}_3$,^[114] $\text{KYF}_4:\text{Yb}/\text{Er}@\text{KYF}_4$,^[50] $\text{YOF}:\text{Yb}/\text{Er}@\text{YOF}$,^[65] $\text{NaYF}_4:\text{Tm}@\text{CaF}_2$,^[101] $\text{NaYF}_4:\text{Yb}/\text{Er}@\text{CaF}_2$,^[115] and $\text{NaYF}_4:\text{Yb}/\text{Tm}@\text{NaYF}_4:\text{Yb}/\text{Er}$ ^[104] have been fabricated to improve the upconversion efficiency. The most important advantage of this strategy is that it provides a simple yet efficient way to enhance the emission intensity of UCNPs in water or biological fluids by protecting the luminescent ions from vibrational deactivation from solvents. This is very important since most bioapplications of UCNPs require them to disperse in water or biofluids.

Tuning the upconversion emission colors: In recent years, considerable efforts have been devoted to tune upconversion emissions over a broad spectral range for applications in multicolor labeling and multiplexed biodetection.^[116] The conventional strategies for tuning the color output of UCNPs typically involve manipulating dopant/host combinations and dopant concentrations. For example, several groups reported a general and versatile approach to fine-tune the upconversion emission colors of Yb/Er and Yb/Tm co-doped UCNPs, such as NaYF_4 , $\text{Na}_x\text{ScF}_{3+x}$ and BaYF_5 .^[47,56,117] By adjusting the different combinations of Tm and/or Er dopants and dopant concentration, the UCL emissions could be readily tuned from UV-visible to NIR under 980 nm excitation. Although different dopant-host combinations can lead to multiple UCL emissions, the color output produced by this method is limited and has several apparent drawbacks. For example, UCNPs show a limited number of efficient emission colors since only three activators (Tm^{3+} , Er^{3+} , and Ho^{3+} ions) are available for generating upconversion emissions.

To broaden the emission color of UCNPs, fluorescence resonance energy transfer (FRET) system based on UCNPs (donors) and organic dyes (acceptors) have been com-

monly employed for modulating the UCL spectra. For example, Li et al. synthesized multicolor upconversion nanocomposites by encapsulating organic dyes or QDs in the silica shell of the core-shell $\text{NaYF}_4:\text{Yb}/\text{Er}(\text{Tm})$ nanospheres.^[116] The as-prepared nanocomposites emitted abundant NIR-to-vis upconversion fluorescence which was generated based on FRET from NaYF_4 nanospheres to the organic dyes or QDs. Similarly, Cheng et al.^[118] reported that modulated UCL emission spectra could be obtained by FRET from the UCNPs to the organic dyes which loaded in amphiphilic polymer on the surface of UCNPs. However, in some case, this strategy still have some drawbacks. For example, the dyes are loaded onto the UCNPs through physical interaction that is sensitive to the environment. This will limit their *in vivo* applications since they may not be stable in physiological condition.

Alternatively, Liu et al.^[119] recently developed a novel intra-particle FRET system for upconversion multicolor fine-tuning by utilizing core-shell nanostructure. They showed that by controlling gadolinium sublattice-mediated energy migration through a well-defined core-shell structure, Ln ions (Tb^{3+} , Eu^{3+} , Dy^{3+} and Sm^{3+}) without long-lived intermediary energy states can serve as the activators to generate tunable upconversion emissions spanning the visible spectral region (Figure 4). The core-shell structure separates the Yb/Tm pair from the activators and eliminates deleterious cross-relaxation. These results indicate that nanostructure engineering is a powerful and versatile route to tune the upconversion emission of UCNPs. Very recently, they proceeded to create a core-shell-shell structure to further enhance the efficiency of activator emission.^[120] They

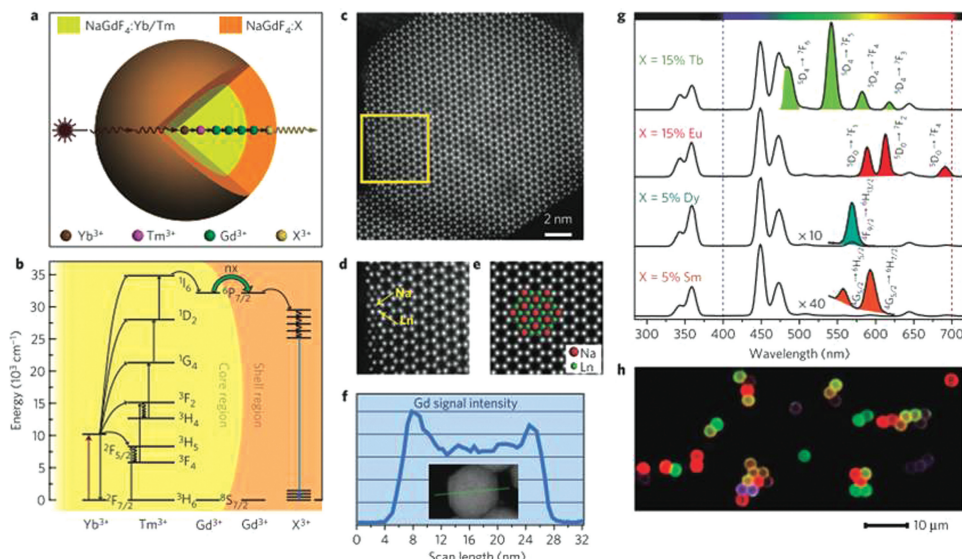


Figure 4. Tuning UCL through energy migration in core-shell nanoparticles: (a) Schematic design of a lanthanide-doped $\text{NaGdF}_4@\text{NaGdF}_4$ core-shell nanoparticle for EMU (X : activator ion). (b) Proposed energy transfer mechanisms. (c) High-resolution STEM image taken at [001] incidence of a nanoparticle comprising a $\text{NaGdF}_4:\text{Yb}/\text{Tm}$ core and a $\text{NaGdF}_4:\text{Tb}$ shell. (d) An enlarged view of the selected area in (c). (e) Digitally processed STEM image. (f) EELS line scan conducted with STEM imaging (inset) on a $\text{NaGdF}_4:\text{Yb}/\text{Tm}@\text{NaGdF}_4:\text{Tb}$ nanoparticle. (g) Emission spectra of the as-prepared $\text{NaGdF}_4@\text{NaGdF}_4$ core-shell nanoparticles doped with different activators. (h) Luminescence micrograph of polystyrene beads tagged with core-shell nanoparticles comprising $\text{NaGdF}_4:\text{Yb}/\text{Tm}@\text{NaGdF}_4$ (blue), $\text{NaGdF}_4:\text{Yb}/\text{Tm}@\text{NaGdF}_4:\text{Tb}$ (green), $\text{NaGdF}_4:\text{Yb}/\text{Tm}@\text{NaGdF}_4:\text{Eu}$ (red), and a binary mixture of $\text{NaGdF}_4:\text{Yb}/\text{Tm}@\text{NaGdF}_4:\text{Tb}$ and $\text{NaGdF}_4:\text{Yb}/\text{Tm}@\text{NaGdF}_4:\text{Eu}$ (yellow), respectively. Adapted with permission.^[119] Copyright 2010, Nature Publishing Group.

found that epitaxial growth of an inert NaYF_4 shell around Ln-doped $\text{NaGdF}_4@\text{NaGdF}_4$ core-shell NPs efficiently prevented the surface quenching of excitation energy, thereby promoting energy transfer to the activators. Thus, various activators (Dy^{3+} , Sm^{3+} , Tb^{3+} and Eu^{3+}) showed clearly enhanced emissions. It is worth noting that the intensity of this kind of UCNPs was almost unchanged in DMSO/ethanol/water owing to the effective protection of activators by the inert shell, facilitating their biological applications. These results are encouraging because they show that for the first time unique properties of UCNPs could be designed and obtained by nanostructure engineering, which is not reproducible in bulk counterparts.

In addition to the multicolor upconversion emissions, single-band UCL with high chromatic purity is also highly desirable. It was reported that, on progressively increasing the dopant concentration of Yb^{3+} , back-energy-transfer from Er^{3+} to Yb^{3+} can be significantly enhanced, thereby resulting in tunable color output of $\text{NaYF}_4:\text{Yb}/\text{Er}$ from yellow to red.^[47] In addition, Yb/Er co-doped UCNPs containing Mn^{2+} ions have shown substantially enhanced red/green emission ratios.^[28] The existence of Mn^{2+} ions disturbs the transition possibilities between green and red emissions of Er^{3+} and facilitates the occurrence of red emission, resulting in an emission color output from green to red by rational controlling the Mn-doping level (Figure 5). Liu and co-workers employed KMnF_3 as the

host material and obtained high pure single-band upconversion emissions from Er^{3+} , Ho^{3+} and Tm^{3+} dopants, respectively, in the red (650 nm) and NIR (800 nm) spectral regions, as a result of the efficient energy transfer between Mn^{2+} and dopant ions.^[27] Using YO^{F} ^[65] and NaMnF_3 ^[66] as host material can also obtain the strong red single-band emissions from Er/Yb dopants. Such single band feature makes it particularly attractive as an ideal optical bioprobe for deep-tissue imaging without the constraints associated with multi-peak UCNPs.

It should be noted that the most of previous efforts were mainly restricted to enhance the UCL intensity or tune the emission colors. It is still a challenge to tune the excitation band of UCNPs. To date, NIR laser at a wavelength of about

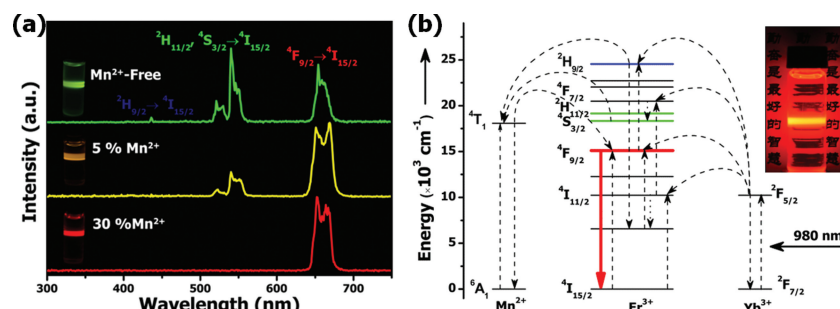


Figure 5. Emission color fine-tuning through Mn^{2+} ions doping: (a) Room temperature upconversion emission spectra of $\text{NaYF}_4:\text{Yb}/\text{Er}$ nanocrystals with 0, 5 and 30 mol% Mn^{2+} dopant ions, respectively; inset: Luminescent photographs of the corresponding samples. (b) Schematic energy level diagram showing the possible upconversion mechanism of Mn^{2+} -doped $\text{NaYF}_4:\text{Yb}/\text{Er}$ nanocrystals. Inset: the bright red emission could lighten the background. Adapted with permission.^[28]

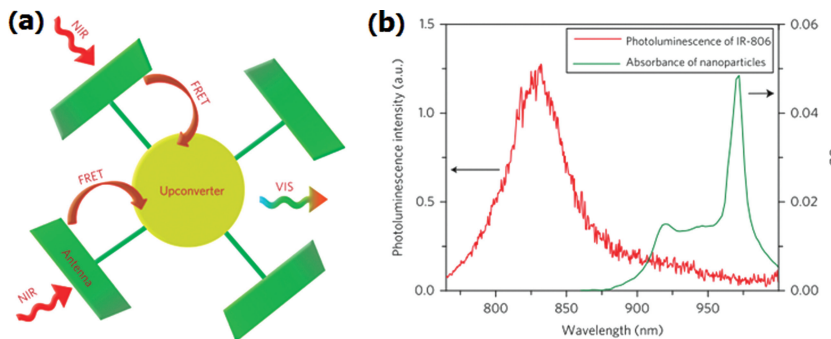


Figure 6. Upconversion goes broadband: (a) Principal concept of the dye-sensitized nanoparticle. Antenna dyes (green) absorb NIR solar energy (red wavy arrows) and transfer it (brown arrows) to the nanoparticle core (in yellow), where upconversion occurs. Upconversion denotes a nonlinear (on the incident radiation intensity) process in which the energies of two NIR quanta are summed to emit a quantum of higher energy in the green-yellow region (green-yellow wavy arrow). (b) Emission spectrum of IR-806 in CHCl_3 (3.18×10^{-6} M; red line) and absorption spectrum of oleylamine-coated $\beta\text{-NaYF}_4\text{:Yb/Er}$ in CHCl_3 (green line). Adapted with permission.^[122] Copyright 2010, Nature Publishing Group.

980 nm is always used to excite UCNPs for upconversion emission since the sensitizer ion Yb^{3+} has a high absorption cross-section in this absorption band. However, the light around 980 nm as excitation source for bioimaging has an intrinsic disadvantage because water in biotissue has a big absorption peak around 980 nm. This disadvantage often causes strong water absorption and sample overheating, which could degrade image resolution, limit the penetration depth of light, and possibly result in substantial cell and tissue damage. Therefore, tuning the excitation band of UCNPs into an appreciate range is also an important issue for improving the performance of UCNPs. He et al.^[121] reported that using a 915 nm CW laser instead of 980 nm light could reduce the radiation heating and increase the penetration depth of light. Recently, Zou and colleagues^[122] developed a new strategy that enabled a broadband excitation of NaYF_4 UCNPs by using organic dye molecules as sensitizers (Figure 6). In their study, NIR dyes were bound to the surface UCNPs, and acted as an antenna to harvest the NIR photons with a broad band (740–850 nm). Then this energy was transferred to Yb^{3+} ions and subsequently transferred to Er^{3+} ions, resulting in a distinctive upconverted emission from the Er^{3+} ions. The overall upconversion emission sensitized by organic dyes was dramatically enhanced (~3,300 times) because of increased absorptivity and overall broadening of the absorption spectrum of the upconverter. Therefore, this work inspires us that tuning the absorption spectrum of the UCNPs is an alternative and significant way to get better performance of UCNPs.^[123]

2.4. Toxicity Studies of Upconversion Nanoparticles

The potential toxicity and biocompatibility of UCNPs are of great importance for their biomedical applications. Similar to many other inorganic NPs, UCNPs could not be easily biodegraded. Thus, the well understanding the behaviors of UCNPs in biological systems as well as their toxicology profiles, is a critical fundamental question to be addressed in order to use

this class of nanomaterials in medical applications in the future. Toxicity considerations should be integrated into materials selection since elements with nontoxicity profile are most likely accepted for biomedical applications. Therefore, NaYF_4 based UCNPs are most investigated since yttrium has an innocuous toxicity profile. Manganese is another essential trace element in human bodies, but its tolerable limit is lower than that of yttrium. Other elements such as Gd^{3+} ions are toxic, which necessitates proper coatings or chelating when they are used *in vivo*.

To date, various cell lines have been used to evaluate the cytotoxicity of different UCNPs through the CCK-8, MTT and MTS assays.^[6,27,34,54,60,73,82,95,124–130] Most of the results suggested that UCNPs were non-cytotoxic to a broad range of tested cell lines within a certain range of concentrations and a limited incubation period. The spatiotemporal distribution of UCNPs in individual living HeLa cells was also investigated by the fluorescence imaging technique.^[131]

The particles were internalized through endocytosis, transported by microtubule-dependent motor proteins (dyneins), accumulated at the perinuclear region, transported by another type of motor proteins (kinesins), and finally released out of the cells. As one of the simplest multicellular eukaryotic organisms with a nervous system, *Caenorhabditis elegans* (*C. elegans*) have also been used as a model organism for evaluating the toxicity of UCNPs. Lim's group,^[132] Yan's group^[133] and Xu's group^[134] reported *in vivo* toxicity studies with the feeding of UCNPs in the *C. elegans* in several aspects, such as the ingestion and excretion of UCNPs, life span, egg viability, the growth rate of UCNPs-treated worms, and so on. Moreover, their results indicated that UCNPs were not significantly toxic except at high concentrations of 10 mg/mL or higher.

The toxicity of UCNPs performed *in vivo* was also assessed through animal studies. For further applications of UCNPs in bioscience and medicine, the most important issue is still the potential long-term toxicity concern of UCNPs and their nanocomposites. It is well known that the long-term toxicity of UCNPs in small animals can be assessed by body weight measurement, histology analysis, serum biochemistry assays, etc. Many groups have reported that the UCNPs treated mice could survive for more than one month without any apparent adverse effects to their health.^[34,69,135,136] To investigate their biocompatibility and tissue distribution, healthy rats were injected intravenously with PAA-UCNPs.^[135] Biodistribution results showed that the uptake and retention of PAA-UCNPs took place primarily in the liver and the spleen. Most of the PAA-UCNPs were excreted from the body of mice in a very slow manner. In addition, histological, hematological and biochemical analysis results indicated that there was no apparent toxicity of PAA-UCNPs in mice at long exposure times (up to 115 days). We also evaluated *in vivo* toxic effects of Gd/Mn contained UCNPs using male and female mice.^[28,137] Thirty days after injection, the survival rate of the mice was 100%. And the weights of the mice did not lose obviously. These results indicated that

Gd/Mn contained UCNPs were low toxicity even Gd/Mn was usually considered as toxic elements. The reason for its low toxicity may be that the Gd³⁺/Mn²⁺ ions were confined in a rigid matrix of host nanocrystals and not easy to be released to the environment. This has been confirmed by inductively coupled plasma mass spectrometry (ICP-MS) analysis. However, to ensure the suitability of the UCNPs for *in vivo* biological applications, further long-term (up to several months) toxicity studies concerning particle size, shape, and surface chemistry are necessary.

3. Surface Functionalization of Upconversion Nanoparticles

Biomedical applications require the UCNPs to be properly coated by hydrophilic and biocompatible agents to render them water-soluble. Besides, the surface coating will bring additional benefits including: (i) significantly preventing the UCNPs from agglomeration in physiological environment; (ii) effectively shielding the UCNPs core against the attack of chemical species in the aqueous solution since the outer coating shell could act as a barrier; (iii) potentially providing functional groups (e.g. amine, carboxyl) that can serve as anchor points for further attaching biomolecules, such as folic acid (FA), peptide, protein, DNA, and so on.^[6,138] In addition, the surface chemistry of UCNPs strongly influences their intracellular behaviors, drug loading and release properties, and longevity in blood circulation.

To date, the reported surface coating strategies for UCNPs mainly focus on the silica encapsulation, ligand engineering and hydrophobic interactions.^[14,139] Silica coating is a well-established strategy for surface modification of UCNPs based on the following advantages: (i) Silica is highly biocompatible; (ii) The coated silica shell greatly reduces the potential risk of toxic effect from leaching of lanthanide ions into the body; (iii) Additional functional groups (such as –NH₂) that allow further conjugation with biological moieties could be simultaneously introduced during the coating procedure; (iv) Silica coating can be used to encapsulate both hydrophilic and hydrophobic UCNPs via Stöber method^[140] and reverse-microemulsion method,^[141] respectively. Recently, coating mesoporous silica on the surface of UCNPs has becoming a popular strategy for surface modification of UCNPs via a modified reverse-microemulsion method.^[65] The advantage of this strategy is that porous silica layer not only improves the water-solubility and biocompatibility of UCNPs but also provides the drug loading capability for NPs due to their porous structure. Various functional molecules, such as chemotherapy drugs, PS and organic dyes, could be tightly adsorbed on the surface of UCNPs, making them widely used for drug delivery, PDT and chemical sensors. It is worth noting that for some biological applications such as FRET-based biosensors and PDT, the thickness of the silica layer on the surface of UCNPs should be precisely controlled. The larger layer will block the FRET from the donor (UCNPs core) to the acceptor (photo-responsive molecules) attached on UCNPs surface, which greatly reduce the efficiency of FRET process.

Another important approach to improve the surface chemistry of UCNPs is ligand engineering, which involves ligand

exchange, oxidation of the native ligands and ligand-free synthesis. In the ligand exchange process, original surface-bound inert ligands such as OA or OM would be (at least partially) substituted by more active ligands, such as polyacrylic acid (PAA),^[142] PEG-Phosphate,^[88] hexanedioic acid (HDA),^[143] 6-aminohexanoic acid (AHA),^[144] thioglycolic acid (TGA),^[67] 3-mercaptopropionic acid (3MA),^[145] dimercaptosuccinic acid (DMSA), citrate,^[38] and 10-decanedicarboxylic acid (DDA),^[146] due to the higher chemical affinity of the latter. This surface modification method offers the water-soluble UCNPs which retain their morphology and crystallization. Ligand oxidation reaction is another efficient method to render NPs water-soluble and provide reactive functional groups for subsequent bioconjugation. Ligand molecules containing unsaturated carbon-carbon double bonds could be directly oxidized into carboxylic acid groups, which improve the hydrophilicity of the treated UCNPs.^[147] Alternatively, ligand-free synthesis method based on removing the surface OA ligand by tuning the pH value of the solution could also provide the water-dispersity of UCNPs and the obtained ligand-free UCNPs could be directly decorated with the electronegative groups (such as –COOH, –SH, and –OH) contained hydrophilic and biocompatible molecules for further application.^[77,148] For example, Capobianco et al. reported on the functionalization of ligand-free NaGdF₄:Yb/Er UCNPs with heparin and basic fibroblast growth factor (bFGF). The heparin-bFGF functionalized UCNPs showed specific binding to the cell membrane.

Hydrophobic-hydrophobic interaction is believed to be a useful method for coating UCNPs.^[6] Amphiphilic molecules coating based on hydrophobic-hydrophobic interactions have been approved as an efficient strategy to convert hydrophobic UCNPs to hydrophilic ones. To date, various amphiphilic molecules including DSPE-mPEG,^[121] amphiphilic polymers or surfactants,^[149] and *block*-polymers^[150] have been successfully used for producing water-soluble UCNPs. For examples, Lu et al.^[29] provided a simple and general method for producing biocompatible UCNPs with versatile chemical surface properties via coating UCNPs surface with a monolayer of functional PEGylated phospholipids. These functional groups (e.g. carboxylic acid, amine, maleimide, and biotin) of the functionalized UCNPs can be easily conjugated with various biomolecules for specific biomedical applications. Pru'homme et al. reported the *block*-copolymer (PEG-b-PLA) modified OA-coated NaYF₄:Yb/Er exhibited excellent stability in water, PBS buffer, and culture medium containing serum proteins.^[151] Our group adopted a commercially available amphiphilic surfactant (TWEEN) as the stabilizer to produce water-soluble and biocompatible UCNPs.^[149] TWEEN compounds are composed of three chemical parts: aliphatic ester chains that can prevent nonspecific adsorption of protein, three-terminal hydroxyl groups that are hydrophilic and can be chemically modified for further applications, as well as an aliphatic chain that can easily be adsorbed on the hydrophobic surface of UCNPs by hydrophobic interactions. This structure makes TWEEN unique for coating UCNPs to render them water-solubility for use in biomedical applications. It is worth mentioning that, the amphiphilic molecule coated UCNPs do not show notable reduction in the overall luminescence intensity compared to the original OA-capped UCNPs. The reason for less quenching

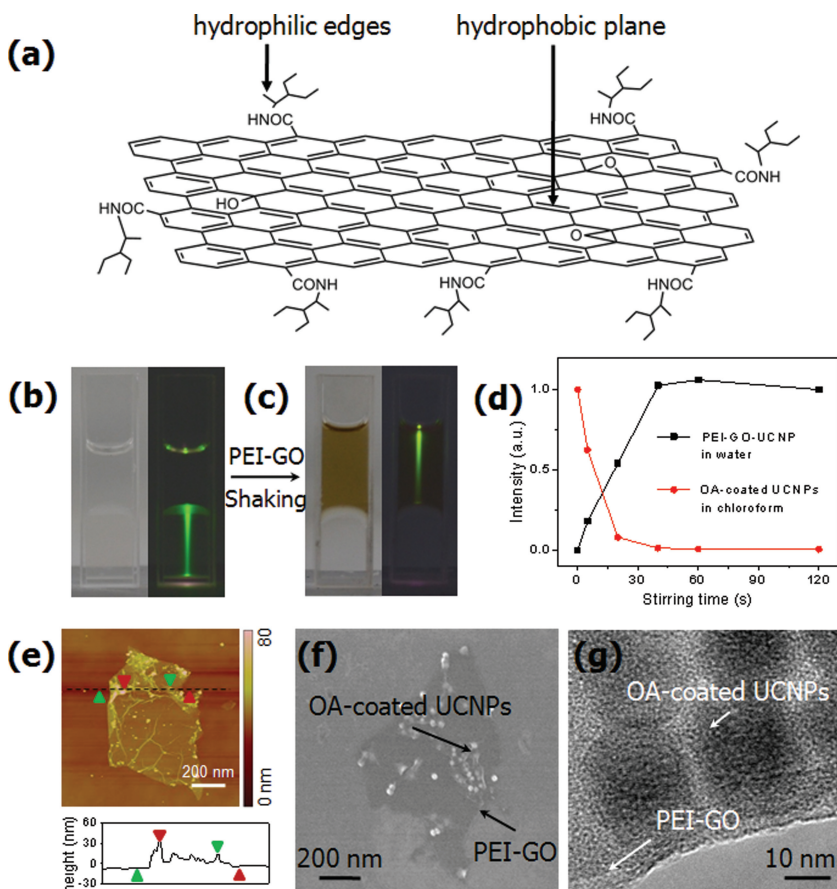


Figure 7. Phase transfer of hydrophobic UCNPs into hydrophilic medium with the assistance of PEI-GO: (a) Model of a PEI functionalized GO nanosheet containing a hydrophobic basal plane and hydrophilic edges. (b) and (c) Photographs of the phase transfer of OA-coated UCNPs_{green} from chloroform to water. The top layers in b and c is pure water, and PEI-GO aqueous solution, respectively; (d) UCL intensity of PEI-GO-UCNP in aqueous phase and OA-coated UCNPs in chloroform; (e) AFM image of PEI-GO-UCNP with a height profile; SEM (f) and TEM (g) images of PEI-GO-UCNP. Adapted with permission.^[130] Copyright 2013, Elsevier.

of upconversion emission in water after amphiphilic molecule coating may be that the hydrophobic layer on the surface of the UCNPs restricted the access of water molecules to the emitting Ln ions resulting in significantly less quenching when compared with UCNPs modified by ligand exchange. Apart from using amphiphilic molecules, we also developed an alternative strategy that used graphene oxide (GO) sheets as nanoscale carriers to transfer the hydrophobic UCNPs to hydrophilic ones.^[130] GO is composed of two parts: largely hydrophobic basal plane and hydrophilic edges, which make them amphiphilic. The basal plane can easily absorb the hydrophobic molecules and nanocrystals through hydrophobic-hydrophobic interactions, while the oxygen-containing functional groups on the edges of GO are able to greatly improve the dispersion of GO in aqueous solution. Therefore, GO could be used for loading hydrophobic UCNPs and rendering them water-soluble, and then building a multifunctional nanoplateform for using in biomedical applications. (Figure 7).

Alternatively, some new methods based on “click” chemistry,^[152] layer-by-layer (LBL),^[153] and host-guest self-assembly^[154–156] are also attractive for UCNPs surface

modification. For example, the “click” reaction, otherwise known as the Huisgen ligation, involves the dipolar cycloaddition of an organic azido group to an alkyne group. The functionalized UCNPs can be further conjugated with functional groups, such as (strept)avidin (via the biotin group) and thiols (via the maleimide (MA) groups). LBL approach based on electrostatic attraction between oppositely charged species permits the preparation of coated colloids of different shapes and sizes, with uniform layers of diverse composition as well as controllable thickness. Recently, Liu et al.^[153] used the LBL approach to obtain PAH-DMMA-PEG-coated NaYF₄:Yb/Er/Mn UCNPs with photosensitizer (Ce6) loaded in each layer for pH-responsive and dual-modal imaging-guided NIR-excited PDT cancer treatment.

The significance of surface functionalization of UCNPs lies in not only making them water-soluble, but also improving their sensitivity of medical imaging and target-specificity of drug delivery by adding targeting agents on the surface of UCNPs. To date, UCNPs with various functional groups, such as carboxylic ($-COOH$), primary amine and MA groups have been obtained for further conjugation with different targeting ligands including FA,^[13,45,81,157,158] peptide,^[159–161] and antibody.^[162–164] These targeting ligands can therefore provide specific biorecognition of target makers or cells through ligand-acceptor, biotin-avidin or antigen-antibody interactions.

Generally, the introduction of targeting molecules to UCNPs surface is often achieved by the following two ways: (1) 1-ethyl-3-[3-(dimethylaminopropyl)] carbodiimide (EDC) and/or N-hydroxysuccinimide (NHS) coupling chemistry based on the coupling reaction between $-NH_2$ and $-COOH$; (2) the reaction between $-SH$ and MA groups. Li et al. reported FA-conjugated NaYF₄:Yb/Er@SiO₂ for targeted UCL imaging of FR-positive KB cells. Lin et al.^[81] reported the FA-modified hollow structured NaYF₄:Yb/Er UCNPs for targeted cell imaging and anti-cancer drug delivery. Zako et al.^[159] reported the use of hetero-functional PEG containing NHS and MA at the both ends to functionalized amine-terminated Y₂O₃:Er@SiO₂ UCNPs to form MA-modified UCNPs. Subsequently, the thiolated c(RGDyK) was grafted onto the MA-modified UCNPs for targeted U87MG cancer cell imaging. Song et al.^[165] reported that the NiNTA conjugation to the NaGdF₄:Yb/Er(Tm) NPs was achieved by using a bifunctional linker (sulfo-SMCC) and then used a site-specific nanoprobe for oligohistidine. Cao et al.^[166] reported the development of neurotoxin-mediated upconversion nanoprobes based on the chlorotoxin (CTX) peptide NaYF₄:Yb/Er/Ce UCNPs for tumor targeting and visualization in living animals. Zhang et al.^[167] utilized the anti-Her2 antibody conjugated NaYF₄:Yb/Er@SiO₂ NPs for targeted UCL imaging of SK-BR-3

and delivering GL3 siRNA to SK-BR-3 cells. Xing et al.^[161] reported Ppa and c(RGDyK) co-modified chitosan-wrapped NaYF₄:Yb/Er UCNPs for targeted near-infrared photodynamic therapy.

4. Applications of Upconversion Nanoparticles for *in vivo* Bioimaging

4.1. *In vivo* Deep Tissue Upconversion Luminescence Imaging and Multicolor Upconversion Luminescence Imaging with Upconversion Nanoparticles

Due to their high penetration depth, low autofluorescence from biosamples, and excellent resistance to photobleaching, UCNPs are highly suitable as luminescent labels for deep-tissue *in vivo* bioimaging. Zhang et al.^[168] first demonstrated the effectiveness of using the PEI-coated NaYF₄:Yb/Er NPs for animal imaging *in vivo* and exhibited the deeper-tissue imaging advantages over QDs. In a later work, Liu et al.^[126] compared the *in vivo* imaging sensitivity of UCNPs and QDs (QD545 and QD625) side by side and demonstrated the *in vivo* detection limit of UCNPs to be at least one order of magnitude lower than that of QDs. To further increase the penetration depth of UCL imaging, tuning the upconversion emission into NIR spectral range (700–1100 nm) and the red light region (600–700 nm) is essential for the deep tissue imaging since the light scattering, absorbance and autofluorescence of tissue in those range are minimum. In a recent work by our group, we reported the single-band red-emitting Mn-doped NaYF₄:Yb/Er UCNPs for *in vivo* imaging and extended the imaging depth to 15 mm.^[28] Besides, Prasad et al.^[125] provided a new approach for *in vivo* imaging by utilizing near infrared to near infrared (NIR-to-NIR) NaYF₄:Yb/Tm as the probe. High-contrast photoluminescence imaging was obtained in mice since both the excitation and emission of the UCNPs used in this work are in the NIR region. From then, NIR-to-NIR UCL from Yb/Tm co-doped UCNPs has been popular as the detection signal and successful UCL imaging of whole-body small animals with light penetration depth up to 20 mm in mouse has been achieved.^[61,98] Moreover, PAA-NaLuF₄:Yb/Tm UCNPs as optical bioprobe has been used *in vivo* UCL imaging of a normal black mouse, even rabbit with excellent signal-to-noise ratio.^[127]

It is well known that multiplexed imaging is a useful strategy for simultaneous recognition of different organisms. With the rapid development in UCNPs design and fabrication, the UCL emission spectra of NPs could be well tuned, thus enabling them for multicolor UCL imaging. Wang et al.^[169] represented the first study of *in vivo* multicolor imaging by using NaYF₄:Yb/Er/La nanorods. Cheng et al.^[126] have reported that three kinds of PEGylated UCNPs with different UCL emission spectra were subcutaneously injected into a rat, and then could be easily differentiated after spectral deconvolution. FRET is

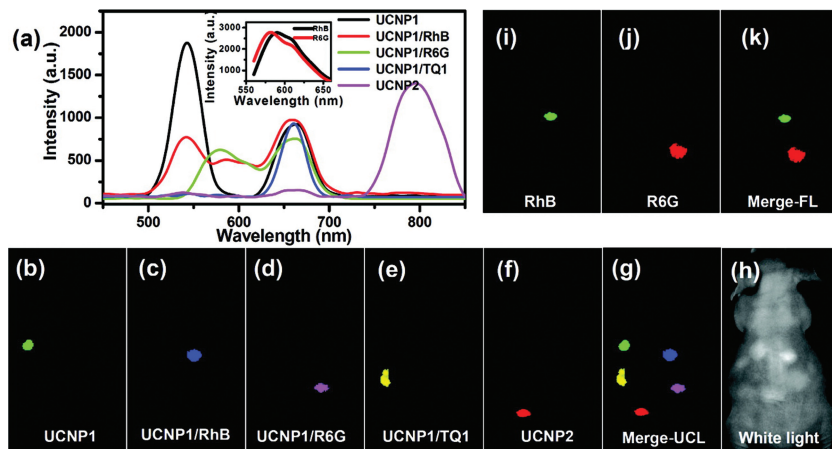


Figure 8. Multicolor *in vivo* UCL imaging of LRET-tuned UCNPs in mice: (a) UCL emission spectra of solutions of UCNP1, UCNP2, UCNP1/RhB, UCNP1/R6G and UCNP1/TQ1 under 980-nm NIR laser excitation. Insert: Fluorescence spectra of RhB and R6G under green light excitation. (b-g) *In vivo* multicolor UCL images of a nude mouse subcutaneously injected with five colors of UCNPs solutions after spectral unmixing. Different colors were individually separated in (b-f) and merged in (g). (h) A white light image of the imaged mouse. (i-k) *In vivo* multicolor down-conversion fluorescence images of the mouse under green light excitation. Adapted with permission.^[118] Copyright 2011, American Chemical Society.

another approach to modulate the UCL spectra of UCNPs for multicolor imaging. The UCL was generated based on FRET from the UCNPs core to organic dyes or QDs around the UCNPs, making these materials with different UCL 'colors' rather useful for *in vitro* and *in vivo* imaging. In the work of Liu group,^[118] they reported that PEGylated UCNPs physically loaded with organic dyes via hydrophobic force could show tuned visible emission spectra owing to the FRET from UCNPs to the organic dyes under NIR excitation, and thus could be serve as a FRET nanosystem for *in vivo* multicolor UCL imaging (Figure 8). Additionally, Kim et al.^[170] have recently demonstrated multiplexed imaging complementarily using QDs and NaYF₄:Yb/Tm NPs by alternating the excitation wavelengths and unmixing the emissions of different probes.

4.2. Upconversion Nanoparticles for Multi-Model Bioimaging

UCNPs were developed specifically as optical imaging contrast agents, but new preparation approaches are being developed that incorporate multiple imaging moieties onto the UCNPs for the use in integrated imaging systems since no single modality is perfect and sufficient to obtain all the necessary information. To broaden their application, UCNPs are often modified to be detected by other imaging modalities including MRI, CT, PET and SPECT. These multimodal agents can assist investigators to visualize the UCNPs across different platforms, including MRI, optical, or nuclear imaging systems.

Most popular UCNPs-based multimodal imaging probes are the combinations of MRI and UCL imaging modalities. It is well known that optical imaging provides the high sensitivity and spatial resolution for *in vitro* imaging, but it is limited by its relatively low penetration depth in biological tissues. In contrast to UCL imaging, MRI provides the excellent spatial resolution and high depth for *in vivo* imaging. By combining UCL

and MRI, it is possible to obtain multiple imaging data with taking the advantages of both techniques. Several strategies have been developed to fabricate UCNPs-based multifunctional nanostructures. The first strategy is molecular functionalization. Usually gadolinium chelates, commonly used MRI contrast agents, were introduced to the surface of UCNPs, which provided MRI modality. For example, Li et al.^[171] reported a core-shell hybrid NPs composed of an UCNPs core and a paramagnetic Gd complex shell. The second one is to combine UCNPs with other magnetic nanostructures by sequential growth or coating. Superparamagnetic iron oxide nanoparticles (SPIONs) have been widely applied in MRI due to their special magnetic properties and good biocompatibility. Currently, some prototypes of UCNPs coupled with SPIONs as dual functional probes have been demonstrated. For example, Li et al.^[172] reported that NaYF₄:Yb/Tm@Fe_xO_y core-shell nanostructure could be acted as an imaging agent for T₂ MRI and UCL dual-modal lymphatic imaging. However, the intensity of UCL emission in this kind of structure will be reduced since the Fe₃O₄ shell absorbs both excitation and emission light. Therefore, they further prepared a different core-shell nanostructure with Fe₃O₄ NPs as core and UCNPs as shell to avoid the absorption by Fe₃O₄.^[36] Very recently, Liu et al.^[173,174] developed a LBL method to prepare UCNPs-SIONPs based nanocomposites which were consisted a UCNPs as the core, a layer of ultra-small iron oxide NPs as the intermediate shell, and a thin layer of gold as the outer shell. Those NPs were used for UCL/MRI dual model bioimaging as well as magnetically targeted photothermal ablation of cancer *in vitro* and *in vivo*. They further employed these nanocomposites for *in vivo* multi-modal labeling, tracking, and manipulation of stem cells. These results showed the promising application of UCNPs-SIONPs as novel multifunctional probes to track and control the translocation of cells *in vivo*.^[139] In addition, constructing the core-shell structure with Gd-based nanoshell onto the surface of UCNPs is also a useful method to prepare magnetic/luminescent dual model probes. For example, by using NaGdF₄ nanostructure as the shell, a series of NaGdF₄:Er/Yb(Tm)@NaGdF₄,^[175] NaYF₄:Yb/Er@NaGdF₄,^[176] and NaYbF₄:Tm@NaGdF₄^[177] nanocomposites were synthesized, which showed good UCL emission and high MRI relaxivity.

However, introducing two or more kinds of NPs into one nano-system is difficult and may cause some unwanted side-effects (for example, Fe₃O₄ may quench the fluorescent materials). From this point of view, Gd-based UCNPs (Gd₂O₃, GdPO₄, GdF₃, NaGdF₄, etc.) are attractive promising single-phase multifunctional bioprobes that present the combination of magnetic and optical properties within one particle.^[33,54,76,113,137,165,178,179] For example, we have demonstrated the successful formation of size tunable Ln-doped Gd₂O₃ NPs with novel multicolor UCL and MRI capabilities.^[137] Unlike other nanocomposites showing multimodality, Gd₂O₃ doped with Ln ions work on their own without adding any other functional moieties. Li et al.^[136] also reported that Yb/Er(Tm) co-doped NaGdF₄ NPs could be used as dual-modal bioprobes for the application in UCL and MRI bioimaging of small animals. Another efficient strategy for the fabrication of single-phase dual MRI/UCL agents is doping magnetic ions (Gd³⁺ or Mn²⁺) into the hosts. For example, we reported that Mn-doped

NaYF₄:Yb/Er nanocrystals displayed UCL emission and magnetic properties.^[28] Zeng et al.^[37] reported that Gd/Yb/Er co-doped NaLuF₄ nanocrystals presented not only efficient NIR to NIR emission but also excellent paramagnetic properties at room temperature. Thus, these bi-functional NaLuF₄ UCNPs have the potential for *in vitro* and *in vivo* dual-modal UCL and MR imaging.

The doping method is also an efficient method for combining other imaging modalities with UCNPs. For example, ¹⁸F is the most widespread radionuclide used in PET imaging for clinical diagnosis. Since the most host materials for UCNPs are fluorides, ¹⁸F can be easily introduced into UCNPs to render them with both UCL and PET imaging modality. Recently, Li et al.^[68] have reported ¹⁸F-labeled NaYF₄:Yb/Tm NPs for dual-modality UCL and PET imaging of whole-body small animals. During the imaging process, the UCNPs could be real-time tracked with high sensitivity *in vivo* from mice to large animals by PET imaging. However, the half-life of ¹⁸F is too short (1.829 h) that greatly limits its biological applications in long-term imaging. To overcome this problem, the same group further prepared ¹⁵³Sm-labeled NaLuF₄:Yb/Tm NPs for UCL and SPECT dual-modality imaging.^[39] The half-life of ¹⁵³Sm (46.3 h) is much longer compared to ¹⁸F. In addition, it also emits medium-energy beta rays, making it suitable for long-term SPECT imaging. These radioactive/upconversion luminescent NaLuF₄:¹⁵³Sm/Yb/Tm NPs have been applied for SPECT and UCL dual-modality bioimaging *in vivo* (**Figure 9**). The biodistribution of the NaLuF₄:¹⁵³Sm/Yb/Tm NPs has been quantified *in vivo* using SPECT bioimaging.

Recently, the applications of UCNPs for tri-modal bioimaging such as PET/MRI/UCL or CT/MRI/UCL are also becoming popular because the combination of different imaging methods enhances their advantages and improves the quality of *in vivo* bioimaging and the efficiency of diagnosis. For example, CT is an efficient non-invasive clinical diagnosis technique that could give high-resolution 3D structure details of tissues based on their differential X-ray absorption. However, owing to the low sensitivity to soft tissues, its applications in disease detection have been greatly limited. MRI can provide unsurpassed 3D soft tissue details and functional information. However, this technique suffers from the limited planar resolution and is not suitable for cellular level imaging. These problems can be solved by fluorescent imaging. Therefore, a synergistic combination of UCL, CT and MRI contrast agents in single system may combine the advantages of each, while avoid their disadvantages. Gd-, Yb-, and Lu-doped/contained nanostructures could be used as excellent CT contrast agents due to their stronger X-ray attenuation and higher atomic number than those of routinely used small iodinated molecules. Up to now, several groups have reported the synergistic combination of UCL, CT and MRI contrast agents in a single system to combine the advantages of each one. Liu et al.^[34] have constructed a multifunctional nanoprobe based on PEGylated Gd₂O₃:Yb/Er nanorods for *in vivo* UCL, MRI, and CT multi-modality imaging. Small-animal experiments indicated that PEGylated Gd₂O₃:Yb/Er nanorods had the capability to be used as high-performance contrast agents to provide diagnostic, therapeutic, as well as prognostic information about the status of disease. Alternatively, Li et al.^[180] designed and prepared Gd-complex modified NaLuF₄-based upconversion

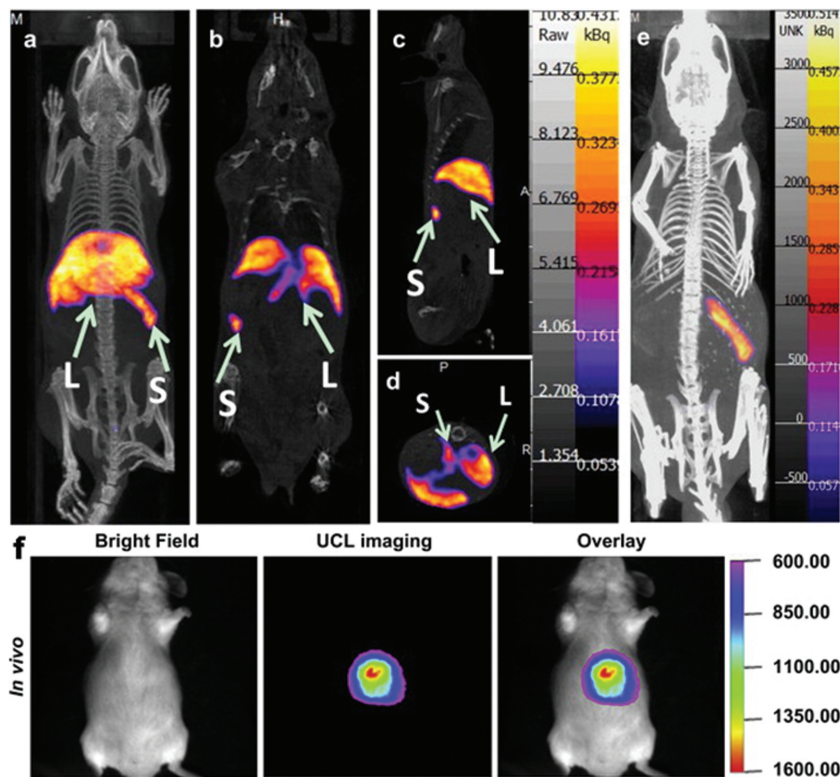


Figure 9. *In vivo* SPECT and UCL imaging study after intravenous injection of ^{153}Sm -UCNPs. (a) whole-body three-dimensional projection, (b) coronal, (c) sagittal and (d) transversal images acquired at 1 h and (e) whole-body three-dimensional projection images acquired at 24 h are shown respectively. The arrows inset point to the liver (L) and spleen (S). (f) *In vivo* UCL imaging of the Kunming mouse 1 h after tail vein injection of the ^{153}Sm -UCNPs (20 mg/kg). Adapted with permission.^[39] Copyright 2013, Elsevier.

nanophosphors for tri-modality imaging of UCL, CT and MRI. Core-shell $\text{Fe}_3\text{O}_4@\text{NaLuF}_4:\text{Yb}/\text{Er}(\text{Tm})$ ^[36] and $\text{NaYF}_4:\text{Yb}/\text{Er}/\text{Tm}@\text{NaGdF}_4@\text{TaO}_x$ ^[7] nanocomposites also have been served as a MRI, CT and UCL bioprobe for tri-modality imaging. Similarly, Li's group developed a cation-assisted ligand assembly method which provided UCNPs with T_1 -magnetic properties by loading Gd^{3+} onto the surface, radioactivity by introducing ^{18}F into the UCNPs, and targeted recognition properties by adsorbing FA on their surfaces.^[181] The functionalized UCNPs can be applied as a tri-modality probe to cellular targeted UCL, MRI and PET imaging. Later, the same group further prepared ^{18}F -labeled $\text{NaYF}_4:\text{Gd}/\text{Yb}/\text{Er}$ NPs with radioactive, magnetic and UCL properties.^[38] Their effectiveness as a multifunctional nanoprobe was evaluated by *in vitro* UCL imaging and *in vivo* MRI/PET bioimaging. Very recently, Os (II) complex-loaded $\text{NaYF}_4:\text{Yb}/\text{Tm}$ nanocomposites are also developed for tri-modal UCL/fluorescence/PET imaging.^[154]

5. Applications of Upconversion Nanoparticles for Cancer Therapy

The application of UCNPs can be further expanded beyond medical imaging by incorporating multifunctionality. A common example is that UCNPs can serve as carriers for

delivering therapeutic payloads, such as photosensitizers (PSs), conventional anti-cancer drugs, therapeutic peptides, proteins and genes. UCNPs-based drug delivery systems retain the ability for monitoring the route of drug-transport carriers and evaluating the efficiency of the drug release in living system by a real-time, simple, and effective way. Here we primarily profile the recent development of UCNPs as carriers for chemotherapy drugs/gene delivery and NIR controlled drug/gene release. We also summarize the exploration of UCNPs for NIR triggered photodynamic cancer therapy.

5.1. Upconversion Nanoparticles for Drug and Gene Delivery

Currently, UCNPs with different nanostructures have been exploited as nanocarriers for loading of various chemotherapy drugs including taxol acid,^[44] doxorubicin (DOX),^[43,63,81] ibuprofen (IBU),^[42,182] and biomolecules.^[183] To successfully integrate a drug into a NP system, several design strategies can be explored, mainly including physical absorption by porous nanostructure and hydrophobic interaction with hydrophobic drug.

In recent years, UCNPs with hollow or mesoporous structures have attracted considerable attention and been commonly used as ideal carriers for drug delivery mainly due to their high specific surface area and cavity

volumes. For example, we reported a multifunctional drug carrier system by encapsulating ibuprofen (IBU) into the uniform $\text{Gd}_2\text{O}_3:\text{Yb}/\text{Er}$ hollow spheres with a mesoporous shell.^[42] Stucky et al.^[184] reported the "nanorattle" spheres consisted of $\text{NaYF}_4:\text{Yb}/\text{Er}$ shells with a moveable SiO_2 -coated Fe_3O_4 inner particle for targeted chemotherapy (Figure 10). Additionally, $\text{Yb}(\text{OH})\text{CO}_3@\text{YbPO}_4:\text{Er}$ and $\text{NaREF}_4:\text{Yb}/\text{Er}$ (RE = Yb, Lu, Y) hollow spheres also have potential for drug loading and then delivery into cancer cells to induce cell death.^[63,80] Mesoporous-structured UCNPs also have been considered to be another excellent candidate as carriers for drug delivery. Lin et al. demonstrated that the core-shell structured $\text{Fe}_3\text{O}_4@\text{nSiO}_2@\text{mSiO}_2@\text{NaYF}_4:\text{Yb}/\text{Er}(\text{Tm})$,^[185] $\text{NaYF}_4:\text{Yb}/\text{Er}@$ silica fiber,^[186] $\text{NaYF}_4:\text{Yb}/\text{Er}@\text{nSiO}_2@\text{mSiO}_2$,^[182] and $\text{Gd}_2\text{O}_3:\text{Er}@\text{nSiO}_2@\text{mSiO}_2$ ^[187] nanocomposites were feasible to act as drug storage carriers and had a controlled drug release property. However, mesoporous silica coating will largely increase the size of NPs since the thickness of m-SiO₂ layer is hard to be controlled within 10 nm so far.

Apart from silica encapsulation, hydrophobic interaction is another simple and efficient way for drug loading on the surface of UCNPs. Unlike silica encapsulation method, this strategy will not notably increase the size of UCNPs. Amphiphilic molecules modified UCNPs have a thin hydrophobic layer on the surface of inorganic NPs that allows the tight attraction

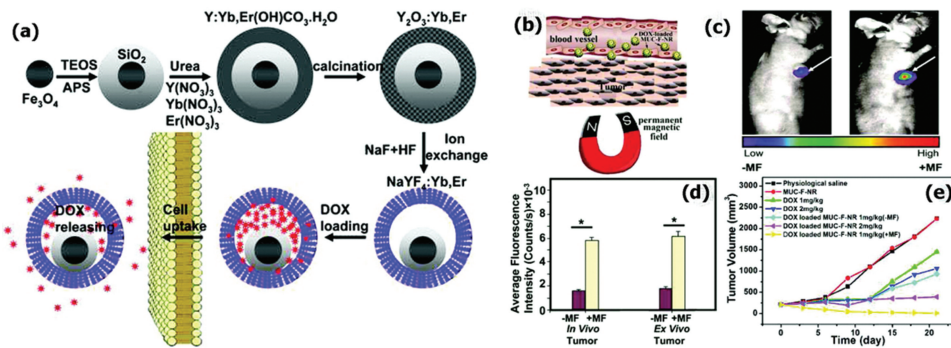


Figure 10. Multifunctional upconversion luminescent and magnetic “nanorattle” materials for targeted chemotherapy: (a) Synthetic procedure for the drug-loaded $\text{Fe}_3\text{O}_4@\text{SiO}_2@ \alpha\text{-NaYF}_4\text{-Yb/Er}$ nanorattles (DOX-MUC-F-NR). (b) Schematic illustration of targeting of DOX loaded multifunctional drug carrier to tumor cells assisted by an externally applied magnetic field (MF). (c) *In vivo* mice imaging. Mice bearing H22 xenograft tumor injected with DOX-MUC-F-NR (1 mg/kg) were subjected (+MF) or not subjected (-MF) to the magnetic field for 1 h before being imaged. (d) The luminescence signal was measured from the whole tumor *in vivo* and *ex vivo*. (e) Tumor volume changes of mice under different treatments. Adapted with permission.^[184] Copyright 2012, American Chemical Society.

of lipophilic molecules. So hydrophobic drugs could be introduced into this layer through hydrophobic interactions. For instance, Liu et al.^[188] reported the employment of PEGylated UCNPs as drug delivery carriers. They showed that a commonly used chemotherapeutic drug, DOX, could be physically adsorbed on the surface of PEGylated UCNPs via hydrophobic interactions. Targeted drug delivery was also realized by conjugating UCNPs with FA targeting moieties (Figure 11). It is worth noting that the release of DOX from UCNPs could be controlled by varying pH values of the environment solution since the interaction between the loaded molecules and UCNPs

is sensitive to environmental conditions. DOX becomes more hydrophilic and water-soluble at low pH value owing to the accelerated protonation of the $-\text{NH}_2$ group in DOX chemical structure, thus leading to the release of more free DOX molecules. The pH-dependent drug release of DOX from UCNPs is of practical significance for the clinical cancer therapy since the microenvironments in extracellular tissues of tumors and intracellular lysosomes and endosomes are acidic.

The major advantage of utilizing UCNPs as drug/gene carriers is that UCNPs have the ability for simultaneously delivering and tracking the intracellular fate of drug/gene or

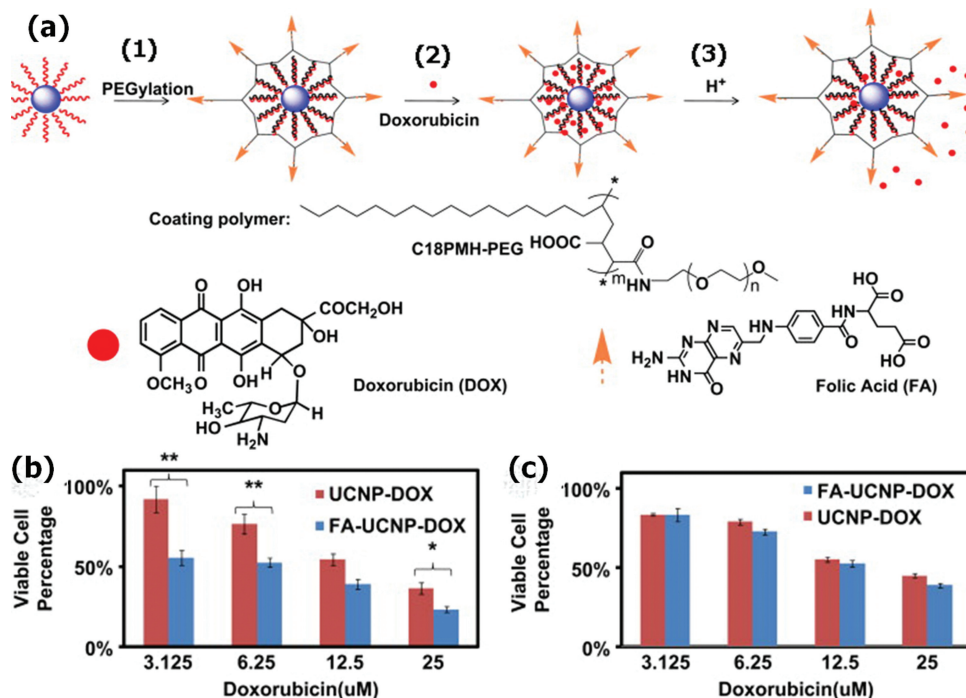


Figure 11. Drug delivery with UCNPs for targeted cancer cell therapy: (a) Schematic illustration of the UCNP-based drug delivery system: (1) OA-capped UCNPs functionalized by C18PMH-PEG-FA; (2) DOX loading on UCNPs through hydrophobic interactions; (3) Release of DOX from UCNPs triggered by decreasing pH. Concentration-dependent cell survival data of (b) FR positive KB cells and (c) negative HeLa cells treated with FA-UCNP-DOX and UCNP-DOX. Adapted with permission.^[188] Copyright 2011, Elsevier.

for imaging-guide therapy. For example, Zhang et al. built a UCNPs-based FRET system for tracking siRNA delivery in live cells.^[189] In this case, UCNPs were denoted as a donor and an intercalating dye (BOBO-3) was chosen as an acceptor. The siRNA-BOBO-3 complexes were physically adsorbed onto the amine-modified NaYF₄:Yb/Er@SiO₂ UCNPs. When the complexes detached from the UCNPs, the efficiency of FRET process would decrease. Intracellular FRET analysis showed that siRNA was gradually released into cells for a duration of 24 h, which was confirmed by confocal microscopy co-localization measurements. The occurrence and disappearance of FRET between UCNPs and dye molecules on siRNA provided an interesting approach to real-time monitor the release and bio-stability of siRNA molecules in live cells.

Very recently, a few "smart" drug delivery systems based on UCNPs have also been fabricated to overcome some drawbacks in the conventional drug carriers. The major drawbacks existed in most conventional drug delivery systems are the irregular drug release due to the variation in physiological conditions and notched distribution of drug in the body leading to adverse reactions. This is a critical problem. For example, antitumor drug delivery systems require "zero-release" before reaching the targeted cells. To overcome these problems, smart drug delivery systems are highly required to regulate the release of the therapeutic payload from a carrier on demand. Light represents the most elegant and non-invasive trigger to deliver bioactive compounds on demand since it allows the accurate control of three

key factors determining the therapeutic outcome, including site, timing and dosage. However, the major hurdle in this process is that photoactivable compounds mostly respond to UV radiation and not to visible or NIR light. This limited the application of caged systems in *in vivo* experiments because of the low level of tissue penetration and phototoxic effects associated with such a short excitation wavelength range. Recent breakthroughs in the fabrication of UCNPs have opened intriguing prospects in photocaging systems. As mentioned above, UCNPs have the unique ability to absorb NIR light and emit UV light locally, which could activate the caged compounds and thereby control the drug release/gene expression under NIR excitation, overcoming the current limitations of using UV irradiation as the stimuli. To date, by using NIR-to-UV UCNPs, a few smart strategies have been developed to control the drug release and gene expression through NIR irradiation.

Recently, Zhang et al.^[190] designed a novel strategy to remotely control gene expression by encapsulating photocaged DNA/siRNA molecules into the porous silica shell of the mesoporous silica-coated NaYF₄:Yb/Tm UCNPs, which provided an improved biocompatibility and increased payload capacity, thus offering a more efficient loading and delivery of the DNA/siRNA cargo (Figure 12). Under NIR excitation, those UCNPs emitted UV light that then could activate these photocaged plasmid DNA or siRNA to induce specific gene expression or down-regulation, respectively. Compared to traditional light-controllable gene therapy using UV light, the use of UCNPs and

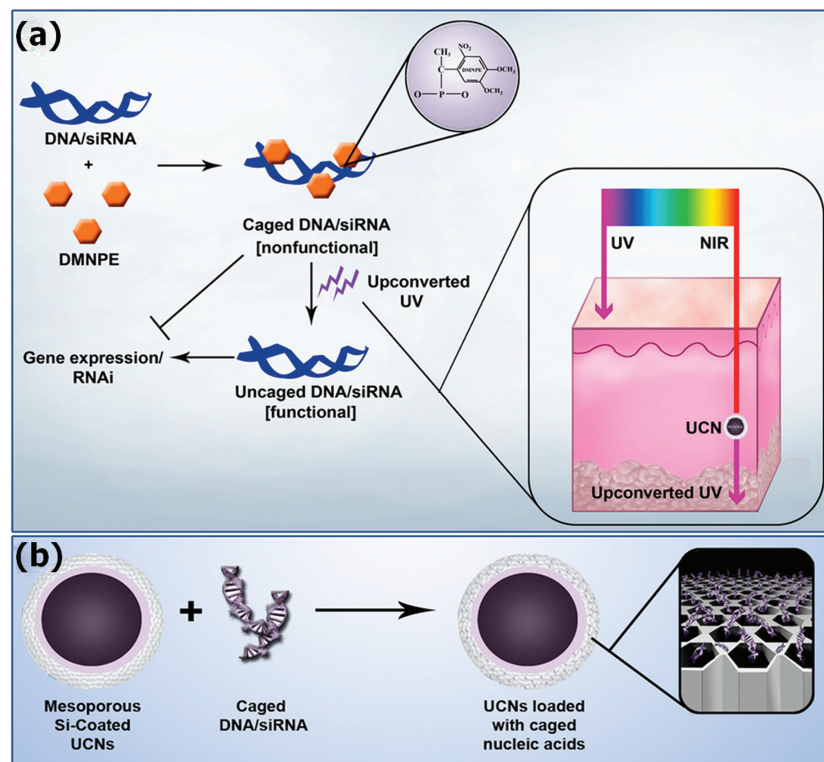


Figure 12. Remote activation of biomolecules in deep tissues using NIR-to-UV upconversion nanotransducers: (a) Plasmid DNA and siRNA are caged with DMNPE and then uncaged by upconverted UV light from NIR-to-UV UCNPs. Inset shows the penetration depth of UV and NIR light in the skin. (b) Loading of caged plasmid DNA/siRNA into the mesopores of UCNPs. Reproduced with permission.^[190] Copyright 2012, National Academy of Science.

NIR excitation is anticipated to increase not only the depth of penetration, but also its associated therapeutic efficiency. Yang et al.^[191] firstly functionalized silica-coated UCNPs by cationic photocaged linkers through covalent bonding. Upon 980-nm laser irradiation, the upconverted UV light could cleave the photosensitive linkers, therefore resulting in the efficient release of siRNA to silence target gene expression in living cells. Similarly, this method was also employed for NIR-triggered release of other caged compound such as NO,^[192] carboxylic acid,^[193] 2-nitrobenzaldehyde^[44] and d-luciferin^[194] by using upconverting nanostructured materials. In addition to photocaged drug delivery system, other photo-responsive systems based UCNPs are also emerging. For example, through using a photosensitive hybrid hydrogel loaded with UCNPs, Yan et al.^[183] showed that NIR light (980 nm) can be employed to induce the gel-sol transition and release large, inactive biomacromolecules (such as protein) into aqueous solution. Very recently, Shi et al.^[195] reported the direct NIR-triggered anticancer drug release based on the mesoporous silica-coated NaYF₄:Yb/Tm@NaYF₄ UCNPs using photoactive moving components, azobenzene groups (azo). Upon NIR irradiation, the upconverted UV light would induce the transformation from *trans* isomer to *cis* isomer form of the photoswitching azo molecules, triggering drug release in a controllable fashion. Therefore, such NIR-to-UV UCNPs have real promise for NIR photo-stimulated delivery of bioactive molecules for therapy and imaging.

5.3. Upconversion Nanoparticles for Photodynamic Therapy

Compared with currently more adopted chemotherapy and radiotherapy, PDT has several unique advantages: cost effectiveness, highly localized and specific tumor treatments, outpatient therapy, higher cure rates, and sparing of extracellular tissue matrix that allows post-PDT regeneration of normal tissue and minimal trauma to organism tissue. However, a major drawback in the current PDT is the requirement of direct illumination of the tissue by visible or even UV light to excite the PS, which has limited penetration depth due to the light absorption and scattering by biological tissues, resulting in ineffective therapeutic efficacy to internal or large tumors. The use of UCNPs as PS carriers provides a potential strategy to overcome the drawbacks of current PDT since they have the ability to convert NIR light to visible photons, which can activate surrounding PS molecules via FRET to generate $^1\text{O}_2$ and kill cancer cells (**Figure 13**).^[12,13,40,41,45,151,153,156,157,161,164,175,196–209] In addition, UCNPs would also facilitate the delivery of PSs since they have better hydrophilicity, appropriate size and targeting molecules for both positive and passive targeting to tumor tissues. (**Table 1**)

Zhang et al.^[197] first demonstrated the application of UCNPs-based PDT in MCF-7/AZ bladder cancer cells. They coated UCNPs with a thin silica layer doped with merocyanine-540. The obtained core-shell NaYF₄:Yb/Er@SiO₂ nanocomposites were functionalized with a tumor targeting anti-body for targeted PDT under NIR light. Nevertheless, the efficiency of PDT in above reports is low because the non-porous silica layer interferes with the diffusion of oxygen molecules from the surrounding environment to the doped PS and the release of the

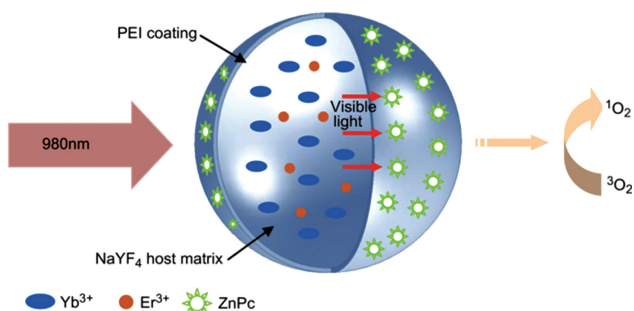


Figure 13. Schematic drawing the mechanism of UCNPs-based PDT: Upon excitation at 980 nm, UCNPs act as nanotransducers by converting NIR light to visible light to excite the nearby ZnPc PSs, which in turn convert the surrounding molecular oxygen to $^1\text{O}_2$. Adapted with permission.^[164] Copyright 2012, Elsevier.

generated reactive oxygen species (ROS).^[175,196,201] To overcome this disadvantage, Chatterjee et al.^[13] and Lim et al.^[164] attached the PS, zinc phthalocyanine (ZnPc), to PEI-modified NaYF₄:Yb/Er UCNPs and used them as nanotransducers for PDT of cancer cells. However, this approach suffers from the low PSs loading efficiency and instability of PS on the UCNPs surface. Moreover, the potential toxicity of PEI hinders their practical PDT application. To further increase the PS concentration and biocompatibility of the UCNPs-PS system, subsequent studies have thus attempted to employ block-copolymer to co-localize PS with UCNPs.^[41,151] Although this method greatly reduced the cytotoxicity and boosted the PS loading, it is hard to determine the optimum ratio between the PS and the UCNPs or release kinetics of the PSs from UCNPs. In view of this, Zhang et al.^[198] coated a mesoporous silica shell onto the surface of UCNPs and loaded ZnPc molecules into this silica layer. They found the ZnPc molecules incorporated into the porous silica shell of UCNPs were not released out of the silica while they continuously produced $^1\text{O}_2$ upon excitation NIR laser. *In vitro* cell treatment demonstrated that the rapid ROS generation and significant cell death were observed under a 500 mW 980-nm laser irradiation for 5 min, indicating an improvement of PDT efficiency. UCNPs with PS molecules incorporated into the mesoporous silica shell have also been developed by a few different groups for NIR light induced PDT, showing encouraging *in vitro* cancer killing results.^[199,204]

The generally adopted encapsulation or adsorption approaches usually suffer from the premature leakage of PS from the nanocarrier. Thus, covalent coupling of PS molecules onto UCNPs should be an ideal strategy for delivering PS. In a recent study, Zhang et al.^[157] developed a covalent bonding strategy to link the Rose Bengal (RB) molecule onto UCNPs. They found that both the PS loading capacity and the energy transfer efficiency from UCNPs to PSs were significantly improved. Specific targeting for folate receptor (FR) positive JAR carcinoma cells was evidenced by UCL cell imaging. After NIR laser irradiation at 1.5 W/cm² for 10 min, cell viabilities decreased significantly for the JAR carcinoma cells but did not obviously change for FR negative noncancerous NIH 3T3 cells. Then, they covalently linked a new PS (monomalic fullerene, C₆₀MA) to the NH₂-functionalized NaYF₄:Yb/Er@NaYF₄:Yb/Tm core-shell UCNPs to construct a highly efficient

Table 1. A summary of published efforts on UCNPs-based photodynamic therapy.

UCNPs (size)	Surface coating	Photosensitizer (Abs_{max})	Conjugated PS to UCNPs	$^1\text{O}_2$ detection marker		Treated cells	Targeting	<i>In vivo</i>	Ref.
				Solution	Intracellular				
NaYF ₄ : Yb/Er (60-120 nm)	Silica	M-540 (555 nm)	Silica encapsulation	ADPA	—	MCF-7/AZ	Yes	No	[197]
NaYF ₄ :Yb/Tm (30-60 nm)	Silica	Ru(bpy) ₃ ²⁺ (450 nm)	Silica encapsulation	ADPA	—	—	—	—	[196]
NaYF ₄ : Yb/Er (ca. 50 nm)	PEI	ZnPc (672 nm)	Coordination	ADPA	—	HT-29	Yes	No	[13]
NaYF ₄ : Yb/Er (ca. 50 nm)	PEI	ZnPc (672 nm)	Coordination	—	—	DENV2-infected HepG2	Yes	Yes	[164]
NaYF ₄ :Yb/Er/Gd (ca. 18 nm) NaYF ₄ :Yb/Er@NaGdF ₄ (ca. 26 nm)	Silica	MB (654 nm)	Silica encapsulation	DPBF	—	—	—	—	[201]
NaGdF ₄ :Yb/Er@NaGdF ₄ (28 ~ 42 nm)	Silica	AlC ₄ Pc (685 nm)	Silica encapsulation	DPBF	—	BNL 1 ME A. 7R.1	No	No	[175]
NaYF ₄ :Yb/Er (ca. 60 nm)	Mesoporous silica	ZnPc (672 nm)	Silica encapsulation	ABDA	—	MB49-PSA	No	No	[198]
NaYF ₄ : Yb/Er (ca. 50 nm)	Mesoporous silica	ZnPc (672 nm)	Silica encapsulation	—	Carboxy-H ₂ DCFDA	MB49-PSA	Yes	No	[199]
NaYF ₄ :Yb/Er (ca. 50 nm)	Mesoporous silica	ZnPc (672 nm)	Silica encapsulation	—	—	MB49-PSA	No	No	[204]
NaYF ₄ : Yb/Er (280 nm)	PEG- <i>b</i> -PCL	TPP (560 nm)	Polymer encapsulation	ADPA	—	—	—	—	[41]
NaYF ₄ : Yb/Er (ca. 100 nm)	PEG- <i>b</i> -PLA	TPP (560 nm)	Polymer encapsulation	—	—	HeLa	No	No	[151]
NaYF ₄ :Yb/Er (ca. 30 nm)	C18PMH-PEG	Ce 6 (663 nm)	hydrophobic interaction	RNO	—	HeLa, 4T1	No	Yes	[200]
NaYF ₄ :Yb/Er (ca. 20 nm)	AEP	RB (550 nm)	Covalent bonding	DPBF	—	NIH 3T3, JAR choriocarcinoma	Yes	No	[157]
NaYF ₄ :Yb/Er@ NaYF ₄ :Yb/Tm (ca. 45 nm)	PAAm	C ₆₀ MA	Covalent bonding	FCLA	—	HeLa, A549	Yes	No	[209]
NaYF ₄ : Yb/Er (ca. 53 nm)	O-Carboxy-methyl chitosan	Ppa (668 nm)	Covalent bonding	FCLA	CM-H ₂ DCFDA	U87-MG, MCF-7	Yes	No	[161]
NaGdF ₄ :Yb/Er@CaF ₂ (ca. 22 nm)	Mesoporous silica	HP (500 nm) SPCD (672 nm)	Covalent bonding	ABMD	—	HeLa	No	No	[206]
NaYF ₄ :Yb/Er (102 ± 23.4 nm)	SOC	ZnPc (672 nm)	SOC encapsulation	DPBF	—	MCF-7	No	Yes	[202]
NaYF ₄ :Yb/Er (ca. 50 nm)	SOC	ZnPc (672 nm)	SOC encapsulation	DPBF	DCFH-DA	HELF, MDA-MB-231	Yes	Yes	[203]
NaYF ₄ :Yb/Er/Mn (ca. 80 nm)	PAH-DMMA-PEG	Ce 6 (663 nm)	Electrostatic adsorption	RNO	—	HeLa, 4T1	No	Yes	[153]
NaYF ₄ :Yb/Er/Mn (20 ~ 30 nm)	α-cyclodextrin	ZnPc (672 nm) Ce 6 (663 nm) MB (654 nm)	Hydrophobic interaction	DPBF	—	A-549	No	No	[156]
NaYF ₄ :Yb/Er@NaGdF ₄ (ca. 42 nm)	(PEG)-phospholipids	Ce 6 (663 nm)	Hydrophobic interaction and covalent bonding	DMA	Carboxy-H ₂ DCFDA	U87MG	No	Yes	[205]
NaYF ₄ : Yb/Er (ca. 100 nm)	Mesoporous silica	M-540 (555 nm) ZnPc (672 nm)	Silica encapsulation	ABDA	Carboxy-H ₂ DCFDA	B16-F0	Yes	Yes	[45]

Abbreviations: ABDA: 9,10-anthracenediyl-bis(methylene)dimalonic acid; ABMD: 9,10-anthracenediylbis-(methylene)dimalonic acid; ADPA: 9,10-anthracenedipropionic acid; AEP: 2-aminoethyl dihydrogen phosphate; AlC₄Pc: Tetrasubstituted carboxy aluminum phthalocyanine; Carboxy-H₂DCFDA: 5-(and 6)-carboxy-2',7'-dichlorodihydrofluorescein diacetate; Ce 6: Chlorin e6; CM-H₂DCFDA: 5-(and-6)-chloromethyl-2',7'-dichlorodihydrofluorescein diacetate, acetyl ester; DCFH-DA: 2',7'-dichlorofluorescein-diacetate. DENV2: Dengue virus serotype-2; DMA: 9,10-dimethylanthracene acid; DPBF: 1,3-diphenylisobenzofuran; FCLA: Fluoresceinyl Cypridina Luciferin Analogue; M-540: Merocyanine-540; HP: hematoporphyrin; MB: Methylene blue; PAAm: poly(allylamine); PEI: Poly(ethylene imine); PEG: poly(ethylene glycol); PEG-*b*-PCL: Poly(ethylene glycol)-block-poly(caprolactone); PEG-*b*-PLA: Poly(ethylene glycol-block-(_{D,L}lactic acid); Ppa: Pyropheophorbide A; RB: Rose Bengal; RNO: p-nitroso-dimethylaniline; Ru(bpy)₃²⁺: Tris(bipyridine)ruthenium(II); SPCD: Silicon phthalocyanine dihydroxide; SOC: N-succinyl-N'-octyl chitosan; TPP: Tetraphenyl porphine; ZnPc: Zinc(II) phthalocyanine.

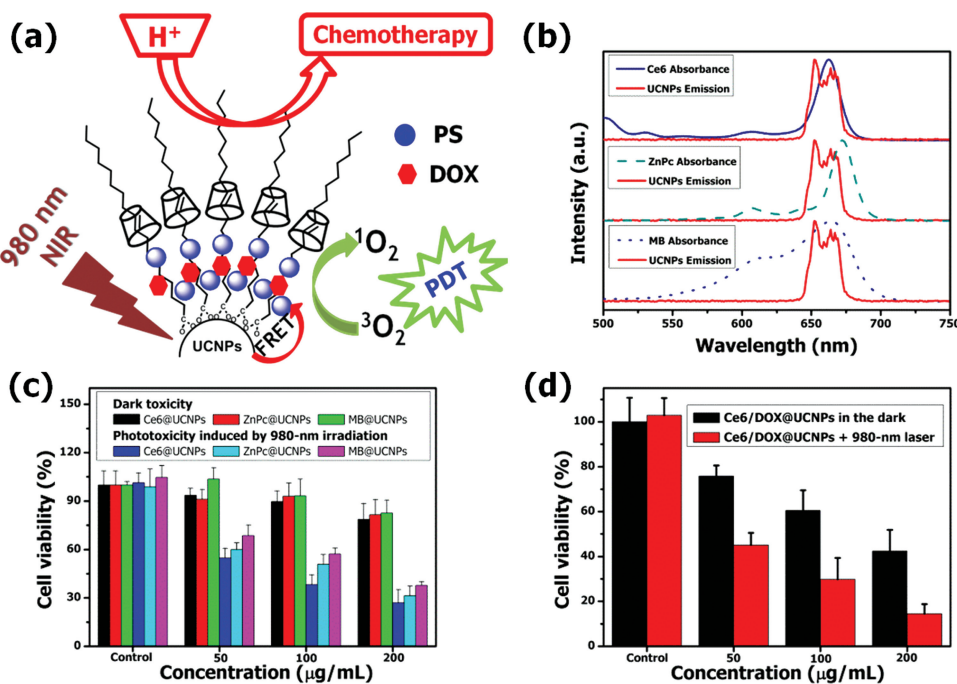


Figure 14. Red-emitting UCNPs-based PDT study: (a) Scheme illustration of the combined therapeutic system for chemotherapy and PDT treatment. b) Spectral overlap between the upconversion emission spectrum of the donor red-emitting $\text{NaYF}_4:\text{Yb}/\text{Er}$ (red solid line) and the absorption spectrum of each acceptor. (c) *In vitro* PDT treatment upon A-549 cancer cells (Power density: 1 W/cm²; Irradiation time: 5 min). (d) Cell killing ability of the combined therapy. Adapted with permission.^[156]

upconversion-C₆₀ nanoplatform for NIR imaging-guided photodynamic therapy of cancer.^[207]

In a recent work reported by our group, a new and efficient NIR photosensitizing nanoplatform for PDT based on single-band red-emitting UCNPs is designed.^[156] In the UCNPs-based phototherapeutic system, cytotoxic $^1\text{O}_2$ is generated through photosensitizing molecules that are activated via FRET process from excited UCNPs. Production of $^1\text{O}_2$ is obviously dependent on the energy transfer efficiency, which relies on the spectral overlap between the UCNPs emission and PS absorption. The red emission band matches well with the efficient absorption bands of the widely used commercially available PSs, benefiting the occurrence of FRET from UCNPs to the attached PSs and thus efficiently activating them to generate $^1\text{O}_2$. In this work, three commonly used PSs, including Ce6, ZnPc and MB, were loaded onto the α -CD-modified red-emitting UCNPs to form PS@UCNPs complexes that efficiently produce $^1\text{O}_2$ to kill cancer cells under 980-nm NIR excitation. Moreover, two different kinds of drugs were co-loaded onto these UCNPs: chemotherapy drug DOX and PDT agent Ce6. The combinational therapy based on DOX-induced chemotherapy and Ce6-triggered PDT exhibited higher therapeutic efficacy relative to the individual means for cancer therapy *in vitro* (Figure 14).

The first *in vivo* UCNP-based PDT study in animal experiments was demonstrated by Liu group.^[200] They non-covalently incorporated Ce6 onto PEGylated UCNPs to form the UCNP-Ce6 nanocomplex as the PDT agent. For animal experiments, UCNP-Ce6 complexes were injected into 4T1 murine breast cancer tumors grown on BALB/C mice. It was found that

70% of tumors were completely eliminated after UCNP-based PDT treatment, without showing re-growth within 2 months. The survival time of mice after UCNP-Ce6 injection and PDT treatment was dramatically prolonged compared to the control mice. Significantly, the NIR light-triggered PDT using UCNP-Ce6 showed a much deeper tissue penetration depth than that of direct excitation by visible light, which was evidenced by both *in vitro* and *in vivo* experiments. These results suggested that UCNP-based PDT induced by NIR light offered remarkably improved tissue penetration depth and could be preferable for the treatment of large or internal tumors. Very recently, they^[153] for the first time realized pH-responsive PDT using PS molecules (Ce6) loaded with charge-reversible UCNPs, for dual-modal imaging-guided NIR-excited PDT cancer treatment. It was found the charge-reversible nanomaterials showed remarkably increased *in vitro* intracellular uptake under acidic cell culture at pH 6.8 and obviously enhanced *in vivo* tumor retention after either intratumor injection or intravenous administration, owing to the slightly acidic tumor microenvironment. Improved PDT cancer killing efficacy under NIR light exposure was proved by both *in vitro* and *in vivo* experiments.

UCNPs-based *in vivo* PDT upon systemic administration was first reported by Hyeon and co-workers.^[205] They developed a novel theranostic probe by attaching Ce6 on PEGylated UCNPs via both physical adsorption and covalent conjugation, obtaining UCNP-Ce6 conjugate as simultaneous *in vivo* dual-modal imaging probes for accurate diagnosis and PDT agents for efficient therapy. Both UCL and MR imaging revealed that UCNP-Ce6 NPs were readily accumulated in the tumor after intravenous injection owing to the enhanced permeability and

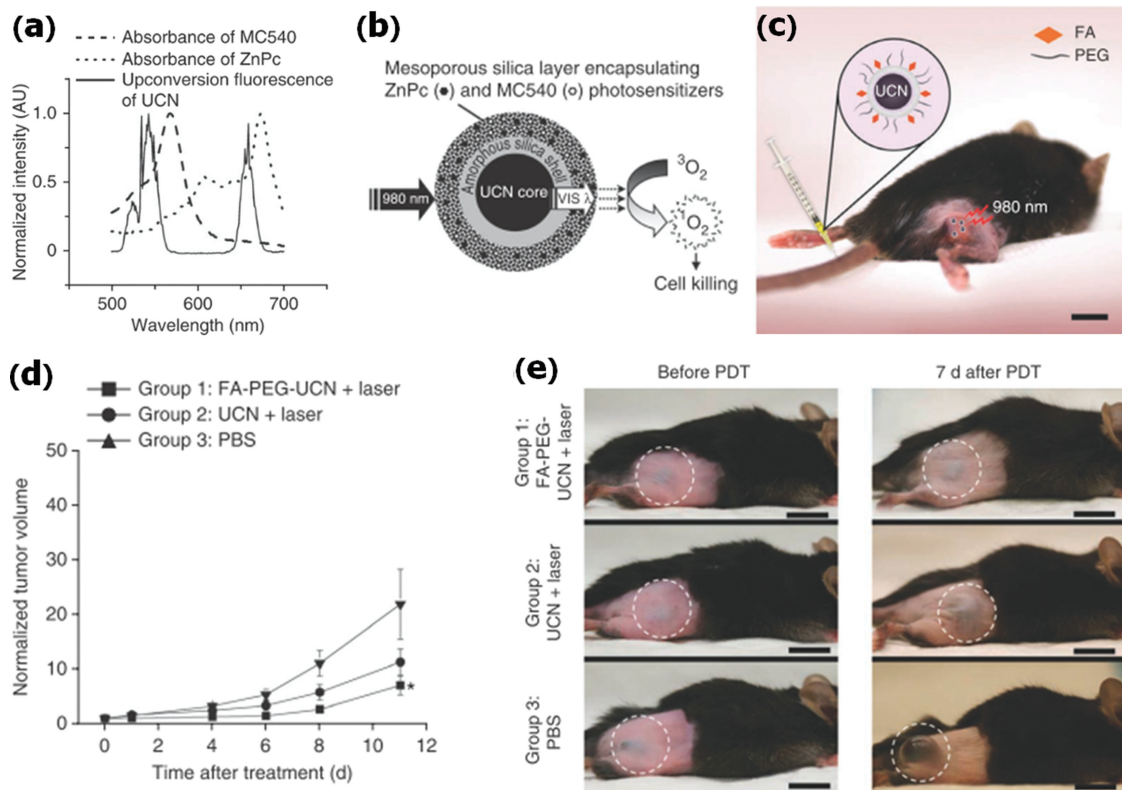


Figure 15. Targeted *in vivo* PDT of a subcutaneous tumor model injected with FA-PEG-UCNPs: (a) The fluorescence emission spectrum of the UCN under 980-nm NIR laser excitation and the absorption spectra of ZnPc and MC540 PSs. AU, arbitrary units. (b) A schematic drawing showing mesoporous-silica-coated UCNPs coloaded with ZnPc and MC540 for PDT. (c) A schematic diagram showing UCNP-based targeted PDT in a mouse model of melanoma. (d) Tumor size Change after various treatments. (e) Representative gross photos of a mouse from each group 1–3 intravenously injected with FA-PEG-UCNs, unmodified UCNs or PBS showing the change in tumor size (highlighted by dashed white circles) before (0 d) and 7 d after PDT treatment. Scale bars, 10 mm. Adapted with permission.^[45] Copyright 2012, Nature Publishing Group.

retention (EPR) effect. Under 980-nm irradiation, the tumor growth on UCN-Ce6 injected mice was significantly inhibited.

To enhance the efficacy of PDT at a single excitation wavelength, Idris et al.^[45] firstly showed a dual-PS loaded UCNPs-based PDT system. Two PSs, ZnPc and merocyanine 540 (MC540), were simultaneous activated by Yb/Er co-doped NaYF₄ under NIR excitation, whose emission peaks (540 nm and 650 nm) overlapped with the absorption peaks of ZnPc and MC 540, respectively (Figure 15). Compared with single-PS loaded UCNP-PS systems, those ZnPc/MC540 co-loaded UCNPs offered greater PDT efficacy, as demonstrated by the enhanced generation of $^1\text{O}_2$ and reduced cell viability after NIR laser irradiation. Importantly, by conjugating ZnPc/MC540 co-loaded UCNPs with FA, *in vivo* targeted PDT treatment of melanoma tumors was demonstrated in their animal experiments, showing notably delayed tumor growth after intravenous injection of UCNPs under NIR laser treatment. This study presented the first proof-of-concept for the UCNPs-based PDT agent for tumor-specific targeted PDT treatment. In another report, Gu et al.^[203] applied the FA-modified chitosan (FASOC) to coat UCNPs and encapsulate ZnPc to constitute tumor-targeted FASOC-UCNP-ZnPc nanoconstructs with high ZnPc loading capacity for deep-penetrating PDT *in vivo*. Their results demonstrated the considerable advantages of tumor-selective

UCNP-based PDT induced by NIR light over traditional PDT for internal tumors.

6. Conclusion and Outlook

We summarized the current research progress of UCNPs in the preparation, surface modification and their applications in bioimaging and cancer therapy. In the past five years, various strategies have been developed to fabricate UCNPs with desired size/shape, efficient upconversion luminescence, and tunable emission colors, as well as other multifunctionalities. Numerous coating strategies, such as ligand engineering and surface encapsulation, have been applied to maximize the stability and biocompatibility of UCNPs systems. The possibility of specific targeting to reach cancer cells or specific tissues is also enabled after the surface modification of UCNPs. By doping/coating multifunctional components into UCNPs, we can create multimodality bioprobes which achieve more sensitive and accurate biomedical imaging meanwhile with multifunction in medical uses. Multifunctional UCNPs systems can deliver the therapeutic drugs with minimized side-effects, while allowing noninvasive monitoring of therapeutic outcome. Nevertheless, many challenges still remain in the field, we highlight some newly emerging ones below.

The first is the safety concern of UCNPs materials in medical uses. In general, the experimental data of cytotoxicity or acute toxicity studies showed signs of less toxicity of the UCNPs. However, from the toxicology viewpoint, the data from *in vivo* cytotoxicity or acute toxicity studies may not reflect to their chronic toxicity *in vivo*. For example, so far, less data for the dose-effect relationship are reported from the toxicity experiments of UCNPs materials, and less data are available for quantitative correlations between UCNPs toxicological properties and their nano-characteristics (e.g., physicochemical properties, size, nanosurface chemistry, nanosurface charge, nanosurface area, nanostructures, shape, morphology, etc.). The lack of the systematically fundamental research of the toxicology aspects of UCNPs may obstruct their medical applications.

The second is how to design the safer UCNPs materials. To minimize the toxicity of UCNPs, we first need the systematical toxicology data for each individual component in UCNPs and also for UCNPs as a whole system. Then, to build a rational surface chemistry for UCNPs becomes the critical aspect.

The third is to exploit the potentials of Ln-doped UCNPs in front of medical sciences such as the newly emerging fields: theranostics, individualized therapeutics, multi-modality medicine, etc. The UCNPs actually provide an ideal multifunctionalized platform that readily meets the requirement of realizing above newly conceptual functions. This needs multidisciplinary collaborative research among chemists, material scientists, biologists, pathologists, clinical doctors, nanotoxicologists, and engineers.

The fourth is how to enhance the quantum yield of UCNPs. This has been discussed in many papers in literature. The UCNPs offer many unique optical properties especially the UCL that makes them suitable for various applications in bio-imaging and bioassay. However, the quantum yield of UCNPs is relative low (usually less than 1%). The fabrication of high efficient UCNPs still remains as a grand challenge. In addition, there are no commercial, ready-to-use instruments in the market for those applications based on UCNPs since most instruments designed according to traditional down-conversion probes that are not suitable for upconversion materials. Similarly, standard measurement equipment and protocols are highly required to allow the quantitative detection of their optical properties.

The fifth is the potential of UCNPs as smart drug delivery system. The UCNPs could harvest the NIR light and then convert it to UV/visible light. This uncommon property makes it becomes a unique transducer to activate photocaged molecules under NIR irradiation. Thus, UCNPs provide a smart platform for create powerful drug delivery systems capable of remotely controlled photorelease of the caged molecules in cells and living animals. However, the development of NIR triggered UCNPs-based drug delivery system is in the infant stage. Many challenges remain when building an efficient and reliable NIR photoactivatable UCNPs-based platform with high loading efficiency for cargos, adequate protection of therapeutic payloads during circulation, target-specific delivery, sufficient cellular internalization, and effective NIR triggered photo-release from UCNPs platform. In addition, the UCNPs-based nanocarriers may also provide imaging tools for real-time monitoring the delivery consequence of the therapeutic payload *in vivo*. With

the help of such a timely on-line information from patients, the clinical doctor can individualize their therapeutic plan for different patients.

Acknowledgements

This work was supported by National Basic Research Programs of China (973 program, No. 2012CB932504, 2011CB933403 and 2013CB933703), and National Natural Science Foundation of China (No. 21001108, 21177128, 21101158, and 21171122).

Received: March 15, 2013

Revised: April 3, 2013

Published online: July 1, 2013

- [1] C. Fang, M. Zhang, *J. Mater. Chem.* **2009**, *19*, 6258.
- [2] J. Kim, Y. Piao, T. Hyeon, *Chem. Soc. Rev.* **2009**, *38*, 372.
- [3] L. Yan, F. Zhao, S. Li, Z. Hu, Y. Zhao, *Nanoscale* **2011**, *3*, 362.
- [4] S. Zeng, K.-T. Yong, I. Roy, X.-Q. Dinh, X. Yu, F. Luan, *Plasmonics* **2011**, *6*, 491.
- [5] J. Xie, G. Liu, H. S. Eden, H. Ai, X. Chen, *Acc. Chem. Res.* **2011**, *44*, 883.
- [6] J. Zhou, Z. Liu, F. Li, *Chem. Soc. Rev.* **2012**, *41*, 1323.
- [7] Q. Xiao, W. Bu, Q. Ren, S. Zhang, H. Xing, F. Chen, M. Li, X. Zheng, Y. Hua, L. Zhou, W. Peng, H. Qu, Z. Wang, K. Zhao, J. Shi, *Biomaterials* **2012**, *33*, 7530.
- [8] L. Feng, L. Wu, X. Qu, *Adv. Mater.* **2013**, *25*, 168.
- [9] L. Cheng, C. Wang, Z. Liu, *Nanoscale* **2013**, *5*, 23.
- [10] O. Veiseh, J. W. Gunn, M. Zhang, *Adv. Drug Delivery Rev.* **2010**, *62*, 284.
- [11] P. Yang, S. Gai, J. Lin, *Chem. Soc. Rev.* **2012**, *41*, 3679.
- [12] D. Bechet, P. Couleaud, C. Frochot, M.-L. Viriot, F. Guillemin, M. Barberi-Heyob, *Trends Biotechnol.* **2008**, *26*, 612.
- [13] D. K. Chatterjee, Z. Yong, *Nanomedicine* **2008**, *3*, 73.
- [14] H. S. Mader, P. Kele, S. M. Saleh, O. S. Wolfbeis, *Curr. Opin. Chem. Biol.* **2010**, *14*, 582.
- [15] C. Bouzigues, T. Gacoin, A. Alexandrou, *ACS Nano* **2011**, *5*, 8488.
- [16] F. Wang, D. Banerjee, Y. Liu, X. Chen, X. Liu, *Analyst* **2010**, *135*, 1839.
- [17] L. H. Fischer, G. S. Harms, O. S. Wolfbeis, *Angew. Chem. Int. Ed.* **2011**, *50*, 4546.
- [18] H. Guo, S. Sun, *Nanoscale* **2012**, *4*, 6692.
- [19] M. Lin, Y. Zhao, S. Wang, M. Liu, Z. Duan, Y. Chen, F. Li, F. Xu, T. Lu, *Biotechnol. Adv.* **2012**, *30*, 1551.
- [20] V. J. Pansare, S. Hejazi, W. J. Faenza, R. K. Prud'homme, *Chem. Mater.* **2012**, *24*, 812.
- [21] K. Kuningas, T. Ukonaho, H. Päkkilä, T. Rantanen, J. Rosenberg, T. Lövgren, T. Soukka, *Anal. Chem.* **2006**, *78*, 4690.
- [22] P. L. A. M. Corstjens, M. Zuiderwijk, H. J. Tanke, J. J. van der Ploeg-van Schip, T. H. M. Ottenhoff, A. Geluk, *Clin. Biochem.* **2008**, *41*, 440.
- [23] O. Ehlert, R. Thomann, M. Darbandi, T. Nann, *ACS Nano* **2008**, *2*, 120.
- [24] H. M. Kim, B. R. Cho, *Acc. Chem. Res.* **2009**, *42*, 863.
- [25] D. K. Chatterjee, M. K. Gnanasammandhan, Y. Zhang, *Small* **2010**, *6*, 2781.
- [26] P. L. A. M. Corstjens, C. J. de Dood, J. J. van der Ploeg-van Schip, K. C. Wiesmeijer, T. Riuttamäki, K. E. van Meijgaarden, J. S. Spencer, H. J. Tanke, T. H. M. Ottenhoff, A. Geluk, *Clin. Biochem.* **2011**, *44*, 1241.
- [27] J. Wang, F. Wang, C. Wang, Z. Liu, X. Liu, *Angew. Chem. Int. Ed.* **2011**, *50*, 10369.

- [28] G. Tian, Z. Gu, L. Zhou, W. Yin, X. Liu, L. Yan, S. Jin, W. Ren, G. Xing, S. Li, Y. Zhao, *Adv. Mater.* **2012**, *24*, 1226.
- [29] L.-L. Li, R. Zhang, L. Yin, K. Zheng, W. Qin, P. R. Selvin, Y. Lu, *Angew. Chem. Int. Ed.* **2012**, *51*, 6121.
- [30] D. Achatz, R. Ali, O. Wolfbeis, in *Luminescence Applied in Sensor Science*, Vol. 300 (Eds: L. Prodi, M. Montalti, N. Zaccheroni), Springer, Berlin Heidelberg, Germany **2011**, Ch.98.
- [31] H. H. Gorris, O. S. Wolfbeis, *Angew. Chem. Int. Ed.* **2013**, *52*, 3584.
- [32] S. A. Hilderbrand, R. Weissleder, *Curr. Opin. Chem. Biol.* **2010**, *14*, 71.
- [33] T. Passuello, M. Pedroni, F. Piccinelli, S. Polizzi, P. Marzola, S. Tambalo, G. Conti, D. Benati, F. Vetrone, M. Bettinelli, A. Speghini, *Nanoscale* **2012**, *4*, 7682.
- [34] Z. Liu, F. Pu, S. Huang, Q. Yuan, J. Ren, X. Qu, *Biomaterials* **2013**, *34*, 1712.
- [35] F. Chen, W. Bu, S. Zhang, J. Liu, W. Fan, L. Zhou, W. Peng, J. Shi, *Adv. Funct. Mater.* **2013**, *23*, 298.
- [36] X. Zhu, J. Zhou, M. Chen, M. Shi, W. Feng, F. Li, *Biomaterials* **2012**, *33*, 4618.
- [37] S. Zeng, J. Xiao, Q. Yang, J. Hao, *J. Mater. Chem.* **2012**, *22*, 9870.
- [38] J. Zhou, M. Yu, Y. Sun, X. Zhang, X. Zhu, Z. Wu, D. Wu, F. Li, *Biomaterials* **2011**, *32*, 1148.
- [39] Y. Yang, Y. Sun, T. Cao, J. Peng, Y. Liu, Y. Wu, W. Feng, Y. Zhang, F. Li, *Biomaterials* **2013**, *34*, 774.
- [40] D. K. Chatterjee, L. S. Fong, Y. Zhang, *Adv. Drug Deliver. Rev.* **2008**, *60*, 1627.
- [41] B. Ungun, R. K. Prud'homme, S. J. Budijon, J. Shan, S. F. Lim, Y. Ju, R. Austin, *Opt. Express* **2009**, *17*, 80.
- [42] G. Tian, Z. Gu, X. Liu, L. Zhou, W. Yin, L. Yan, S. Jin, W. Ren, G. Xing, S. Li, Y. Zhao, *J. Phys. Chem. C* **2011**, *115*, 23790.
- [43] Y. Dai, D. Yang, P. Ma, X. Kang, X. Zhang, C. Li, Z. Hou, Z. Cheng, J. Lin, *Biomaterials* **2012**, *33*, 8704.
- [44] N.-C. Fan, F.-Y. Cheng, J. A. Ho, C.-S. Yeh, *Angew. Chem. Int. Ed.* **2012**, *51*, 8806.
- [45] N. M. Idris, M. K. Gnansammandhan, J. Zhang, P. C. Ho, R. Mahendran, Y. Zhang, *Nat. Med.* **2012**, *18*, 1580.
- [46] F. Auzel, *Chem. Rev.* **2004**, *104*, 139.
- [47] F. Wang, X. Liu, *J. Am. Chem. Soc.* **2008**, *130*, 5642.
- [48] F. Wang, X. Liu, *Chem. Soc. Rev.* **2009**, *38*, 976.
- [49] A. Gnach, A. Bednarkiewicz, *Nano Today* **2012**, *7*, 532.
- [50] H. Schäfer, P. Ptacek, O. Zerzouf, M. Haase, *Adv. Funct. Mater.* **2008**, *18*, 2913.
- [51] C. Chen, L.-D. Sun, Z.-X. Li, L.-L. Li, J. Zhang, Y.-W. Zhang, C.-H. Yan, *Langmuir* **2010**, *26*, 8797.
- [52] H. Schäfer, P. Ptacek, H. Eickmeier, M. Haase, *Adv. Funct. Mater.* **2009**, *19*, 3091.
- [53] D. Chen, Y. Yu, F. Huang, Y. Wang, *Chem. Commun.* **2011**, *47*, 2601.
- [54] W. Yin, L. Zhao, L. Zhou, Z. Gu, X. Liu, G. Tian, S. Jin, L. Yan, W. Ren, G. Xing, Y. Zhao, *Chem. Eur. J.* **2012**, *18*, 9239.
- [55] F. Li, C. Li, X. Liu, T. Bai, W. Dong, X. Zhang, Z. Shi, S. Feng, *Dalton Trans.* **2013**, *42*, 2015.
- [56] X. Teng, Y. Zhu, W. Wei, S. Wang, J. Huang, R. Naccache, W. Hu, A. I. Y. Tok, Y. Han, Q. Zhang, Q. Fan, W. Huang, J. A. Capobianco, L. Huang, *J. Am. Chem. Soc.* **2011**, *134*, 8340.
- [57] G. Chen, T. Y. Ohulchanskyy, R. Kumar, H. Ågren, P. N. Prasad, *ACS Nano* **2010**, *4*, 3163.
- [58] H.-T. Wong, F. Vetrone, R. Naccache, H. L. W. Chan, J. Hao, J. A. Capobianco, *J. Mater. Chem.* **2011**, *21*, 16589.
- [59] G. Wang, Q. Peng, Y. Li, *J. Am. Chem. Soc.* **2009**, *131*, 14200.
- [60] N.-N. Dong, M. Pedroni, F. Piccinelli, G. Conti, A. Sbarbati, J. E. Ramírez-Hernández, L. M. Maestro, M. C. Iglesias-de la Cruz, F. Sanz-Rodríguez, A. Juarranz, F. Chen, F. Vetrone, J. A. Capobianco, J. G. Solé, M. Bettinelli, D. Jaque, A. Speghini, *ACS Nano* **2011**, *5*, 8665.
- [61] Q. Liu, Y. Sun, T. Yang, W. Feng, C. Li, F. Li, *J. Am. Chem. Soc.* **2011**, *133*, 17122.
- [62] F. Shi, J. Wang, X. Zhai, D. Zhao, W. Qin, *CrystEngComm.* **2011**, *13*, 3782.
- [63] D. Yang, Y. Dai, P. Ma, X. Kang, Z. Cheng, C. Li, J. Lin, *Chem. Eur. J.* **2013**, *19*, 2685.
- [64] S. Sarkar, B. Meesargandla, C. Hazra, V. Mahalingam, *Adv. Mater.* **2013**, *25*, 856.
- [65] G. Yi, Y. Peng, Z. Gao, *Chem. Mater.* **2011**, *23*, 2729.
- [66] Y. Zhang, J. D. Lin, V. Vijayaragavan, K. K. Bhakoo, T. T. Y. Tan, *Chem. Commun.* **2012**, *48*, 10322.
- [67] D. Chen, Y. Yu, F. Huang, H. Lin, P. Huang, A. Yang, Z. Wang, Y. Wang, *J. Mater. Chem.* **2012**, *22*, 2632.
- [68] Y. Sun, M. Yu, S. Liang, Y. Zhang, C. Li, T. Mou, W. Yang, X. Zhang, B. Li, C. Huang, F. Li, *Biomaterials* **2011**, *32*, 2999.
- [69] Y. Yang, Y. Sun, Y. Liu, J. Peng, Y. Wu, Y. Zhang, W. Feng, F. Li, *Biomaterials* **2013**, *34*, 508.
- [70] Y. Sun, Q. Liu, J. Peng, W. Feng, Y. Zhang, P. Yang, F. Li, *Biomaterials* **2013**, *34*, 2289.
- [71] J. A. Dorman, J. H. Choi, G. Kuzmanich, J. P. Chang, *J. Phys. Chem. C* **2012**, *116*, 10333.
- [72] H. Liang, Y. Zheng, G. Chen, L. Wu, Z. Zhang, W. Cao, *J. Alloy. Compd.* **2011**, *509*, 409.
- [73] W. Yin, L. Zhou, Z. Gu, G. Tian, S. Jin, L. Yan, X. Liu, G. Xing, W. Ren, F. Liu, Z. Pan, Y. Zhao, *J. Mater. Chem.* **2012**, *22*, 6974.
- [74] P. C. de Sousa Filho, O. A. Serra, *J. Phys. Chem. C* **2010**, *115*, 636.
- [75] S. Lee, K. Teshima, S. Mori, M. Endo, S. Oishi, *Crys. Grow. Des.* **2010**, *10*, 1693.
- [76] W. Ren, G. Tian, L. Zhou, W. Yin, L. Yan, S. Jin, Y. Zu, S. Li, Z. Gu, Y. Zhao, *Nanoscale* **2012**, *4*, 3754.
- [77] N. Bogdan, E. M. Rodriguez, F. Sanz-Rodriguez, M. C. Iglesias de la Cruz, A. Juarranz, D. Jaque, J. G. Sole, J. A. Capobianco, *Nanoscale* **2012**, *4*, 3647.
- [78] Y. Song, Y. Huang, L. Zhang, Y. Zheng, N. Guo, H. You, *RSC Adv.* **2012**, *2*, 4777.
- [79] Z. Xu, Y. Cao, C. Li, P. a. Ma, X. Zhai, S. Huang, X. Kang, M. Shang, D. Yang, Y. Dai, J. Lin, *J. Mater. Chem.* **2011**, *21*, 3686.
- [80] Z. Xu, P. Ma, C. Li, Z. Hou, X. Zhai, S. Huang, J. Lin, *Biomaterials* **2011**, *32*, 4161.
- [81] D. Yang, X. Kang, P. a. Ma, Y. Dai, Z. Hou, Z. Cheng, C. Li, J. Lin, *Biomaterials* **2013**, *34*, 1601.
- [82] S. Zeng, M.-K. Tsang, C.-F. Chan, K.-L. Wong, J. Hao, *Biomaterials* **2012**, *33*, 9232.
- [83] Y. Tang, W. Di, X. Zhai, R. Yang, W. Qin, *ACS Catal.* **2013**, *3*, 405.
- [84] F. Wang, D. K. Chatterjee, Z. Li, Y. Zhang, X. Fan, M. Wang, *Nanotechnology* **2006**, *17*, 5786.
- [85] C. Li, Z. Quan, P. Yang, S. Huang, H. Lian, J. Lin, *J. Phys. Chem. C* **2008**, *112*, 13395.
- [86] J. Liu, W. Bu, S. Zhang, F. Chen, H. Xing, L. Pan, L. Zhou, W. Peng, J. Shi, *Chem. Eur. J.* **2012**, *18*, 2335.
- [87] C. Zhang, Z. Hou, R. Chai, Z. Cheng, Z. Xu, C. Li, L. Huang, J. Lin, *J. Phys. Chem. C* **2010**, *114*, 6928.
- [88] J.-C. Boyer, M.-P. Manseau, J. I. Murray, F. C. J. M. van Veggel, *Langmuir* **2009**, *26*, 1157.
- [89] H. Kobayashi, N. Kosaka, M. Ogawa, N. Y. Morgan, P. D. Smith, C. B. Murray, X. Ye, J. Collins, G. A. Kumar, H. Bell, P. L. Choyke, *J. Mater. Chem.* **2009**, *19*, 6481.
- [90] A. Dong, X. Ye, J. Chen, Y. Kang, T. Gordon, J. M. Kikkawa, C. B. Murray, *J. Am. Chem. Soc.* **2010**, *133*, 998.
- [91] X. Ye, J. E. Collins, Y. Kang, J. Chen, D. T. N. Chen, A. G. Yodh, C. B. Murray, *Proc. Natl. Acad. Sci. U S A* **2010**, *107*, 22430.
- [92] M. Sabotakin, X. Ye, S. J. Oh, S.-H. Hong, A. T. Fafarman, U. K. Chettiar, N. Engheta, C. B. Murray, C. R. Kagan, *ACS Nano* **2012**, *6*, 8758.

- [93] H.-X. Mai, Y.-W. Zhang, R. Si, Z.-G. Yan, L.-d. Sun, L.-P. You, C.-H. Yan, *J. Am. Chem. Soc.* **2006**, *128*, 6426.
- [94] Y.-P. Du, Y.-W. Zhang, L.-D. Sun, C.-H. Yan, *J. Phys. Chem. C* **2008**, *112*, 405.
- [95] J.-C. Boyer, F. Vetrone, L. A. Cuccia, J. A. Capobianco, *J. Am. Chem. Soc.* **2006**, *128*, 7444.
- [96] J.-C. Boyer, L. A. Cuccia, J. A. Capobianco, *Nano Lett.* **2007**, *7*, 847.
- [97] V. Mahalingam, F. Vetrone, R. Naccache, A. Speghini, J. A. Capobianco, *J. Mater. Chem.* **2009**, *19*, 3149.
- [98] J. Pichaandi, J.-C. Boyer, K. R. Delaney, F. C. J. M. van Veggel, *J. Phys. Chem. C* **2011**, *115*, 19054.
- [99] A. F. Khan, R. Yadav, P. K. Mukhopadhyay, S. Singh, C. Dwivedi, V. Dutta, S. Chawla, *J. Nanopart. Res.* **2011**, *13*, 6837.
- [100] G. Chen, T. Y. Ohulchansky, S. Liu, W.-C. Law, F. Wu, M. T. Swihart, H. Ågren, P. N. Prasad, *ACS Nano* **2012**, *6*, 2969.
- [101] G. Chen, J. Shen, T. Y. Ohulchansky, N. J. Patel, A. Kutikov, Z. Li, J. Song, R. K. Pandey, H. Ågren, P. N. Prasad, G. Han, *ACS Nano* **2012**, *6*, 8280.
- [102] A. Kar, A. Patra, *Nanoscale* **2012**, *4*, 3608.
- [103] C. Zhang, J. Y. Lee, *ACS Nano* **2013**, *7*, 4393.
- [104] H.-S. Qian, Y. Zhang, *Langmuir* **2008**, *24*, 12123.
- [105] F. Wang, Y. Han, C. S. Lim, Y. Lu, J. Wang, J. Xu, H. Chen, C. Zhang, M. Hong, X. Liu, *Nature* **2010**, *463*, 1061.
- [106] D. Chen, Y. Yu, F. Huang, P. Huang, A. Yang, Y. Wang, *J. Am. Chem. Soc.* **2010**, *132*, 9976.
- [107] D. Chen, P. Huang, Y. Yu, F. Huang, A. Yang, Y. Wang, *Chem. Commun.* **2011**, *47*, 5801.
- [108] N. Liu, W. Qin, G. Qin, T. Jiang, D. Zhao, *Chem. Commun.* **2011**, *47*, 7671.
- [109] H. P. Paudel, L. Zhong, K. Bayat, M. F. Baroughi, S. Smith, C. Lin, C. Jiang, M. T. Berry, P. S. May, *J. Phys. Chem. C* **2011**, *115*, 19028.
- [110] P. Yuan, Y. H. Lee, M. K. Gnanasammudhan, Z. Guan, Y. Zhang, Q.-H. Xu, *Nanoscale* **2012**, *4*, 5132.
- [111] Y. Wang, L. Tu, J. Zhao, Y. Sun, X. Kong, H. Zhang, *J. Phys. Chem. C* **2009**, *113*, 7164.
- [112] F. Zhang, R. Che, X. Li, C. Yao, J. Yang, D. Shen, P. Hu, W. Li, D. Zhao, *Nano Lett.* **2012**, *12*, 2852.
- [113] Y. I. Park, J. H. Kim, K. T. Lee, K.-S. Jeon, H. B. Na, J. H. Yu, H. M. Kim, N. Lee, S. H. Choi, S.-I. Baik, H. Kim, S. P. Park, B.-J. Park, Y. W. Kim, S. H. Lee, S.-Y. Yoon, I. C. Song, W. K. Moon, Y. D. Suh, T. Hyeon, *Adv. Mater.* **2009**, *21*, 4467.
- [114] C. Li, X. Liu, P. Yang, C. Zhang, H. Lian, J. Lin, *J. Phys. Chem. C* **2008**, *112*, 2904.
- [115] Y.-F. Wang, L.-D. Sun, J.-W. Xiao, W. Feng, J.-C. Zhou, J. Shen, C.-H. Yan, *Chem. Eur. J.* **2012**, *18*, 5558.
- [116] Z. Li, Y. Zhang, S. Jiang, *Adv. Mater.* **2008**, *20*, 4765.
- [117] F. Vetrone, V. Mahalingam, J. A. Capobianco, *Chem. Mater.* **2009**, *21*, 1847.
- [118] L. Cheng, K. Yang, M. Shao, S.-T. Lee, Z. Liu, *J. Phys. Chem. C* **2011**, *115*, 2686.
- [119] F. Wang, R. Deng, J. Wang, Q. Wang, Y. Han, H. Zhu, X. Chen, X. Liu, *Nat. Mater.* **2011**, *10*, 968.
- [120] Q. Su, S. Han, X. Xie, H. Zhu, H. Chen, C.-K. Chen, R.-S. Liu, X. Chen, F. Wang, X. Liu, *J. Am. Chem. Soc.* **2012**, *134*, 20849.
- [121] Q. Zhan, J. Qian, H. Liang, G. Somesfalean, D. Wang, S. He, Z. Zhang, S. Andersson-Engels, *ACS Nano* **2011**, *5*, 3744.
- [122] W. Zou, C. Visser, J. A. Maduro, M. S. Pshenichnikov, J. C. Hummelen, *Nat. Photon.* **2012**, *6*, 560.
- [123] X. Xie, X. Liu, *Nat. Mater.* **2012**, *11*, 842.
- [124] R. Abdul Jalil, Y. Zhang, *Biomaterials* **2008**, *29*, 4122.
- [125] M. Nyk, R. Kumar, T. Y. Ohulchansky, E. J. Bergey, P. N. Prasad, *Nano Lett.* **2008**, *8*, 3834.
- [126] L. Cheng, K. Yang, S. Zhang, M. Shao, S. Lee, Z. Liu, *Nano Res.* **2010**, *3*, 722.
- [127] T. Yang, Y. Sun, Q. Liu, W. Feng, P. Yang, F. Li, *Biomaterials* **2012**, *33*, 3733.
- [128] J. Zhou, X. Zhu, M. Chen, Y. Sun, F. Li, *Biomaterials* **2012**, *33*, 6201.
- [129] X. Wei, W. Wang, K. Chen, *Dalton Trans.* **2013**, *42*, 1752.
- [130] L. Yan, Y.-N. Chang, L. Zhao, Z. Gu, X. Liu, G. Tian, L. Zhou, W. Ren, S. Jin, W. Yin, H. Chang, G. Xing, X. Gao, Y. Zhao, *Carbon* **2013**, *57*, 120.
- [131] Y. M. Bae, Y. Park, S. H. Nam, J. H. Kim, K. Lee, H. M. Kim, B. Yoo, J. S. Choi, K. T. Lee, T. Hyeon, Y. D. Suh, *Biomaterials* **2012**, *33*, 9080.
- [132] S. F. Lim, R. Riehn, W. S. Ryu, N. Khanarian, C.-K. Tung, D. Tank, R. H. Austin, *Nano Lett.* **2005**, *6*, 169.
- [133] J.-C. Zhou, Z.-L. Yang, W. Dong, R.-J. Tang, L.-D. Sun, C.-H. Yan, *Biomaterials* **2011**, *32*, 9059.
- [134] J. Chen, C. Guo, M. Wang, L. Huang, L. Wang, C. Mi, J. Li, X. Fang, C. Mao, S. Xu, *J. Mater. Chem.* **2011**, *21*, 2632.
- [135] L. Xiong, T. Yang, Y. Yang, C. Xu, F. Li, *Biomaterials* **2010**, *31*, 7078.
- [136] J. Zhou, Y. Sun, X. Du, L. Xiong, H. Hu, F. Li, *Biomaterials* **2010**, *31*, 3287.
- [137] L. Zhou, Z. Gu, X. Liu, W. Yin, G. Tian, L. Yan, S. Jin, W. Ren, G. Xing, W. Li, X. Chang, Z. Hu, Y. Zhao, *J. Mater. Chem.* **2012**, *22*, 966.
- [138] Y. Huang, S. He, W. Cao, K. Cai, X.-J. Liang, *Nanoscale* **2012**, *4*, 6135.
- [139] L. Cheng, C. Wang, X. Ma, Q. Wang, Y. Cheng, H. Wang, Y. Li, Z. Liu, *Adv. Funct. Mater.* **2013**, *23*, 272.
- [140] C. Mi, Z. Tian, C. Cao, Z. Wang, C. Mao, S. Xu, *Langmuir* **2011**, *27*, 14632.
- [141] J. Shan, Y. Ju, *Appl. Phys. Lett.* **2007**, *91*, 123103.
- [142] R. Naccache, F. Vetrone, V. Mahalingam, L. A. Cuccia, J. A. Capobianco, *Chem. Mater.* **2009**, *21*, 717.
- [143] S. Cui, H. Chen, Y. Gu, *J. Phys. Conf. Ser.* **2011**, *277*, 012006.
- [144] T. Cao, Y. Yang, Y. Gao, J. Zhou, Z. Li, F. Li, *Biomaterials* **2011**, *32*, 2959.
- [145] Z.-L. Wang, J. Hao, H. L. W. Chan, G.-L. Law, W.-T. Wong, K.-L. Wong, M. B. Murphy, T. Su, Z. H. Zhang, S. Q. Zeng, *Nanoscale* **2011**, *3*, 2175.
- [146] J. Shen, L.-D. Sun, Y.-W. Zhang, C.-H. Yan, *Chem. Commun.* **2010**, *46*, 5731.
- [147] Z. Chen, H. Chen, H. Hu, M. Yu, F. Li, Q. Zhang, Z. Zhou, T. Yi, C. Huang, *J. Am. Chem. Soc.* **2008**, *130*, 3023.
- [148] N. Bogdan, F. Vetrone, G. A. Ozin, J. A. Capobianco, *Nano Lett.* **2011**, *11*, 835.
- [149] W. Ren, G. Tian, S. Jian, Z. Gu, L. Zhou, L. Yan, S. Jin, W. Yin, Y. Zhao, *RSC Adv.* **2012**, *2*, 7037.
- [150] S. J. Budijono, J. Shan, N. Yao, Y. Miura, T. Hoye, R. H. Austin, Y. Ju, R. K. Prud'homme, *Chem. Mater.* **2010**, *22*, 311.
- [151] J. Shan, S. J. Budijono, G. Hu, N. Yao, Y. Kang, Y. Ju, R. K. Prud'homme, *Adv. Funct. Mater.* **2011**, *21*, 2488.
- [152] H. S. Mader, M. Link, D. E. Achatz, K. Uhlmann, X. Li, O. S. Wolfbeis, *Chem. Eur. J.* **2010**, *16*, 5416.
- [153] C. Wang, L. Cheng, Y. Liu, X. Wang, X. Ma, Z. Deng, Y. Li, Z. Liu, *Adv. Funct. Mater.* **2013**, *23*, 272.
- [154] Q. Liu, M. Chen, Y. Sun, G. Chen, T. Yang, Y. Gao, X. Zhang, F. Li, *Biomaterials* **2011**, *32*, 8243.
- [155] Q. Liu, C. Li, T. Yang, T. Yi, F. Li, *Chem. Commun.* **2010**, *46*, 5551.
- [156] G. Tian, W. Ren, L. Yan, S. Jian, Z. Gu, L. Zhou, S. Jin, W. Yin, S. Li, Y. Zhao, *Small* **2012**, *9*, 1929.
- [157] K. Liu, X. Liu, Q. Zeng, Y. Zhang, L. Tu, T. Liu, X. Kong, Y. Wang, F. Cao, S. A. G. Lambrechts, M. C. G. Aalders, H. Zhang, *ACS Nano* **2012**, *6*, 4054.
- [158] J. Ma, P. Huang, M. He, L. Pan, Z. Zhou, L. Feng, G. Gao, D. Cui, *J. Phys. Chem. B* **2012**, *116*, 14062.
- [159] T. Zako, H. Nagata, N. Terada, A. Utsumi, M. Sakono, M. Yohda, H. Ueda, K. Soga, M. Maeda, *Biochem. Biophys. Res. Commun.* **2009**, *381*, 54.

- [160] Y. Zhang, F. Zheng, T. Yang, W. Zhou, Y. Liu, N. Man, L. Zhang, N. Jin, Q. Dou, Y. Zhang, Z. Li, L.-P. Wen, *Nat. Mater.* **2012**, *11*, 817.
- [161] A. Zhou, Y. Wei, B. Wu, Q. Chen, D. Xing, *Mol. Pharm.* **2012**, *9*, 1580.
- [162] R. Kumar, M. Nyk, T. Y. Ohulchanskyy, C. A. Flask, P. N. Prasad, *Adv. Funct. Mater.* **2009**, *19*, 853.
- [163] M. Wang, C.-C. Mi, W.-X. Wang, C.-H. Liu, Y.-F. Wu, Z.-R. Xu, C.-B. Mao, S.-K. Xu, *ACS Nano* **2009**, *3*, 1580.
- [164] M. E. Lim, Y.-I. Lee, Y. Zhang, J. J. H. Chu, *Biomaterials* **2012**, *33*, 1912.
- [165] J. Ryu, H.-Y. Park, K. Kim, H. Kim, J. H. Yoo, M. Kang, K. Im, R. Grailhe, R. Song, *J. Phys. Chem. C* **2010**, *114*, 21077.
- [166] X.-F. Yu, Z. Sun, M. Li, Y. Xiang, Q.-Q. Wang, F. Tang, Y. Wu, Z. Cao, W. Li, *Biomaterials* **2010**, *31*, 8724.
- [167] S. Jiang, Y. Zhang, K. M. Lim, E. K. W. Sim, L. Ye, *Nanotechnology* **2009**, *20*, 155101.
- [168] D. K. Chatterjee, A. J. Rufaihah, Y. Zhang, *Biomaterials* **2008**, *29*, 937.
- [169] X. Yu, M. Li, M. Xie, L. Chen, Y. Li, Q. Wang, *Nano Res.* **2010**, *3*, 51.
- [170] S. Jeong, N. Won, J. Lee, J. Bang, J. Yoo, S. G. Kim, J. A. Chang, J. Kim, S. Kim, *Chem. Commun.* **2011**, *47*, 8022.
- [171] Z. Li, Y. Zhang, B. Shuter, N. Muhammad Idris, *Langmuir* **2009**, *25*, 12015.
- [172] A. Xia, Y. Gao, J. Zhou, C. Li, T. Yang, D. Wu, L. Wu, F. Li, *Biomaterials* **2011**, *32*, 7200.
- [173] L. Cheng, K. Yang, Y. Li, J. Chen, C. Wang, M. Shao, S.-T. Lee, Z. Liu, *Angew. Chem. Int. Ed.* **2011**, *50*, 7385.
- [174] L. Cheng, K. Yang, Y. Li, X. Zeng, M. Shao, S.-T. Lee, Z. Liu, *Biomaterials* **2012**, *33*, 2215.
- [175] Z. Zhao, Y. Han, C. Lin, D. Hu, F. Wang, X. Chen, Z. Chen, N. Zheng, *Chem. Asian J.* **2012**, *7*, 830.
- [176] H. Gao, Z. Li, H. Qian, Y. Hu, I. N. Muhammad, *Nanotechnology* **2010**, *21*, 125602.
- [177] G. Chen, T. Y. Ohulchanskyy, W. C. Law, H. Agren, P. N. Prasad, *Nanoscale* **2011**, *3*, 2003.
- [178] G. K. Das, B. C. Heng, S.-C. Ng, T. White, J. S. C. Loo, L. D'Silva, P. Padmanabhan, K. K. Bhakoo, S. T. Selvan, T. T. Y. Tan, *Langmuir* **2010**, *26*, 8959.
- [179] F. Li, C. Li, X. Liu, Y. Chen, T. Bai, L. Wang, Z. Shi, S. Feng, *Chem. Eur. J.* **2012**, *18*, 11641.
- [180] A. Xia, M. Chen, Y. Gao, D. Wu, W. Feng, F. Li, *Biomaterials* **2012**, *33*, 5394.
- [181] Q. Liu, Y. Sun, C. Li, J. Zhou, C. Li, T. Yang, X. Zhang, T. Yi, D. Wu, F. Li, *ACS Nano* **2011**, *5*, 3146.
- [182] X. Kang, Z. Cheng, C. Li, D. Yang, M. Shang, P. a. Ma, G. Li, N. Liu, J. Lin, *J. Phys. Chem. C* **2011**, *115*, 15801.
- [183] B. Yan, J.-C. Boyer, D. Habault, N. R. Branda, Y. Zhao, *J. Am. Chem. Soc.* **2012**, *134*, 16558.
- [184] F. Zhang, G. B. Braun, A. Pallaoro, Y. Zhang, Y. Shi, D. Cui, M. Moskovits, D. Zhao, G. D. Stucky, *Nano Lett.* **2011**, *12*, 61.
- [185] S. Gai, P. Yang, C. Li, W. Wang, Y. Dai, N. Niu, J. Lin, *Adv. Funct. Mater.* **2010**, *20*, 1166.
- [186] Z. Hou, C. Li, P. Ma, G. Li, Z. Cheng, C. Peng, D. Yang, P. Yang, J. Lin, *Adv. Funct. Mater.* **2011**, *21*, 2356.
- [187] Z. Xu, C. Li, P. a. Ma, Z. Hou, D. Yang, X. Kang, J. Lin, *Nanoscale* **2011**, *3*, 661.
- [188] C. Wang, L. Cheng, Z. Liu, *Biomaterials* **2011**, *32*, 1110.
- [189] S. Jiang, Y. Zhang, *Langmuir* **2010**, *26*, 6689.
- [190] M. K. G. Jayakumar, N. M. Idris, Y. Zhang, *Proc. Natl. Acad. Sci. U S A* **2012**, *109*, 8483.
- [191] Y. Yang, F. Liu, X. Liu, B. Xing, *Nanoscale* **2013**, *5*, 231.
- [192] J. V. Garcia, J. Yang, D. Shen, C. Yao, X. Li, R. Wang, G. D. Stucky, D. Zhao, P. C. Ford, F. Zhang, *Small* **2012**, *8*, 3800.
- [193] C.-J. Carling, F. Nourmohammadian, J.-C. Boyer, N. R. Branda, *Angew. Chem. Int. Ed.* **2010**, *49*, 3782.
- [194] Y. Yang, Q. Shao, R. Deng, C. Wang, X. Teng, K. Cheng, Z. Cheng, L. Huang, Z. Liu, X. Liu, B. Xing, *Angew. Chem. Int. Ed.* **2012**, *51*, 3125.
- [195] J. Liu, W. Bu, L. Pan, J. Shi, *Angew. Chem. Int. Ed.* **2013**, *52*, 4375.
- [196] Y. Guo, M. Kumar, P. Zhang, *Chem. Mater.* **2007**, *19*, 6071.
- [197] P. Zhang, W. Steelant, M. Kumar, M. Scholfield, *J. Am. Chem. Soc.* **2007**, *129*, 4526.
- [198] H. S. Qian, H. C. Guo, P. C.-L. Ho, R. Mahendran, Y. Zhang, *Small* **2009**, *5*, 2285.
- [199] H. Guo, H. Qian, N. M. Idris, Y. Zhang, *Nanome. Nanotechnol. Biol. Med.* **2010**, *6*, 486.
- [200] C. Wang, H. Tao, L. Cheng, Z. Liu, *Biomaterials* **2011**, *32*, 6145.
- [201] F. Chen, S. Zhang, W. Bu, Y. Chen, Q. Xiao, J. Liu, H. Xing, L. Zhou, W. Peng, J. Shi, *Chem. Eur. J.* **2012**, *18*, 7082.
- [202] S. Cui, H. Chen, H. Zhu, J. Tian, X. Chi, Z. Qian, S. Achilefu, Y. Gu, *J. Mater. Chem.* **2012**, *22*, 4861.
- [203] S. Cui, D. Yin, Y. Chen, Y. Di, H. Chen, Y. Ma, S. Achilefu, Y. Gu, *ACS Nano* **2012**, *7*, 676.
- [204] X. Liu, H. Qian, Y. Ji, Z. Li, Y. Shao, Y. Hu, G. Tong, L. Li, W. Guo, H. Guo, *RSC Adv.* **2012**, *2*, 12263.
- [205] Y. Park, H. M. Kim, J. H. Kim, K. C. Moon, B. Yoo, K. T. Lee, N. Lee, Y. Choi, W. Park, D. Ling, K. Na, W. K. Moon, S. H. Choi, H. S. Park, S.-Y. Yoon, Y. D. Suh, S. H. Lee, T. Hyeon, *Adv. Mater.* **2012**, *24*, 5755.
- [206] X.-F. Qiao, J.-C. Zhou, J.-W. Xiao, Y.-F. Wang, L.-D. Sun, C.-H. Yan, *Nanoscale* **2012**, *4*, 4611.
- [207] X. Liu, M. Zheng, X. Kong, Y. Zhang, Q. Zeng, Z. Sun, W. J. Buma, H. Zhang, *Chem. Commun.* **2013**, *49*, 3224.
- [208] J. Sun, F. Zhong, X. Yi, J. Zhao, *Inorg. Chem.* **2013**, *52*, 6229.
- [209] Q. Xiao, Y. Ji, Z. Xiao, Y. Zhang, H. Lin, Q. Wang, *Chem. Commun.* **2013**, *49*, 1527.